

Zeitschrift: Eclogae Geologicae Helvetiae
Band: 87 (1994)
Heft: 2: Pollution and pollutant transport in the geosphere, a major environmental issue : symposium held during the 173rd annual meeting of the Swiss Academy of Natural Sciences

Artikel: Repeated change from crustal shortening to orogen-parallel extension in the Austroalpine units of Graubünden
Autor: Froitzheim, Nikolaus / Schmid, Stefan M. / Conti, Paolo
DOI: <https://doi.org/10.5169/seals-167471>

Nutzungsbedingungen

Die ETH-Bibliothek ist die Anbieterin der digitalisierten Zeitschriften. Sie besitzt keine Urheberrechte an den Zeitschriften und ist nicht verantwortlich für deren Inhalte. Die Rechte liegen in der Regel bei den Herausgebern beziehungsweise den externen Rechteinhabern. [Siehe Rechtliche Hinweise.](#)

Conditions d'utilisation

L'ETH Library est le fournisseur des revues numérisées. Elle ne détient aucun droit d'auteur sur les revues et n'est pas responsable de leur contenu. En règle générale, les droits sont détenus par les éditeurs ou les détenteurs de droits externes. [Voir Informations légales.](#)

Terms of use

The ETH Library is the provider of the digitised journals. It does not own any copyrights to the journals and is not responsible for their content. The rights usually lie with the publishers or the external rights holders. [See Legal notice.](#)

Download PDF: 22.11.2024

ETH-Bibliothek Zürich, E-Periodica, <https://www.e-periodica.ch>

Repeated change from crustal shortening to orogen-parallel extension in the Austroalpine units of Graubünden

NIKOLAUS FROITZHEIM, STEFAN M. SCHMID & PAOLO CONTI¹

Dedicated to Prof. Rudolf Trümpy

Key words: Crustal shortening, orogen-parallel extension, structural geology, tectonics, Alps, Austroalpine, Graubünden

Zusammenfassung, Abstract

1 Introduction	561
2 Austroalpine tectonic units in Graubünden and their position in the Jurassic passive continental margin	563
3 Alpine deformation of the southwestern Silvretta, Ela and Err-Carungas nappes	565
3.1 Southwestern Silvretta nappe (Ducan area)	570
3.1.1 General description	570
3.1.2 D ₁ folding and thrusting in the Silvretta nappe	571
3.1.3 D ₂ normal faulting in the Silvretta nappe	571
3.1.4 Fault rocks from the Ducan normal fault and the base of the Silvretta nappe	572
3.1.5 D ₃ folding in the Silvretta nappe	576
3.2 Ela nappe	576
3.2.1 General description	576
3.2.2 D ₁ folding and thrusting in the Ela nappe	577
3.2.3 D ₂ “collapse folding” and minor normal faulting in the Ela nappe	580
3.2.4 D ₃ folding in the Ela nappe	583
3.3 Err-Carungas nappe	584
3.3.1 General description	584
3.3.2 Structural analysis	584
4 Sequence of stages of the orogenic evolution	585
4.1 Trupchun phase (D ₁): Cretaceous top-west thrusting and folding	585
4.2 Ducan-Ela phase (D ₂): Late Cretaceous east-west extension	586
4.3 Blaisun phase (D ₃): Early Tertiary north-south shortening	587
4.4 Turba phase (D ₄): Renewed east-west extension	587
4.5 Domleschg phase (D ₅): Late-stage northwest-southeast shortening	588
5 Comparison with the Engadine Dolomites	588
5.1 General description	589
5.2 Correlation across the Engadine line	589

¹ Geologisch-Paläontologisches Institut der Universität, Bernoullistrasse 32, CH-4056 Basel

5.3	Trupchun-phase folding and thrusting in the Engadine Dolomites	591
5.4	Post-nappe deformation of the Engadine Dolomites	592
6	Synthesis: Structural evolution of the Austroalpine nappes in Graubünden	593
6.1	Cretaceous orogeny	593
6.1.1	From the Jurassic passive margin to the Late Cretaceous thrust belt	593
6.1.2	Sinistral wrench movement along the Albula steep zone	599
6.1.3	Late Cretaceous extension: Collapse behind a migrating orogenic wedge	601
6.2	Tertiary orogeny	603
6.2.1	Early Tertiary collisional deformation	603
6.2.2	Postcollisional deformation of the Austroalpine nappes	604
7	Conclusions	606
	Acknowledgments	607
	References	607

ZUSAMMENFASSUNG

Mit Hilfe einer struktureologischen Analyse der ostalpinen Einheiten in Graubünden wurde die Aufeinanderfolge von zwei orogenen Zyklen, kretazischen und tertiären Alters, nachgewiesen. Beide Zyklen umfassen Überschiebungstektonik, gefolgt von extensionaler Überprägung. Während beider Extensionsphasen, in der späten Kreide und im frühen bis mittleren Oligozän, war die Dehnungsrichtung etwa parallel zum heutigen Streichen des Orogens orientiert.

Die tektonische Entwicklung wird in fünf Phasen eingeteilt: (1) Spätkretazische Deckenstapelung und sinistrale Transpression (Trupchun-Phase). Der ostalpine Deckenstapel entstand durch schräge, westgerichtete Imbrikation des nordwestlichen passiven Kontinentalrandes des apulischen Mikrokontinents, begleitet von sinistraler Transpression an der Ost-West-verlaufenden Albula-Steilzone. (2) Spätkretazische Extension (Ducan-Ela-Phase). Der Deckenstapel wurde durch ost- bis südostgerichtete Abschiebungen überprägt. Gleichzeitig mit bedeutenden flachliegenden Abschiebungen bildeten sich in einem tieferen Stockwerk liegende Falten. Diese Falten entstanden durch Ost-West-Dehnung und vertikale Verkürzung vorher steilstehender Schichten. Abschiebungen und liegende Falten werden deshalb als verschiedene Auswirkungen der gleichen Extensionsphase angesehen. (3) Frühtertiäre Kollisionstektonik (Blaisun-Phase). Die spätkretazischen Extensionsstrukturen wurden durch ost- bis südoststreichende Falten überprägt. Diese entstanden wahrscheinlich während der frühtertiären, nordgerichteten Überschiebung des gesamten ostalpinen Deckenstapels ("orogener Deckel") über die tieferen penninischen Einheiten. (4) Früh- bis mitteloligozäne Extension (Turba-Phase). Diese zweite Episode von Ost-West-Dehnung betraf vor allem die Grenzzone zwischen dem orogenen Deckel und dem unterliegenden Penninikum, und führte lokal zu einer extensionalen Entkoppelung dieser beiden Stockwerke (Turba-Mylonitzone). (5) Spätoligozäne postkollisionale Verkürzung (Domleschg-Phase). Diese letzte Faltenphase der ostalpinen Decken zeigt NW-SE-Verkürzung an.

Im Massstab des gesamten ostalpinen Bereichs gesehen, migrierten sowohl die kretazische Verkürzung als auch die darauffolgende spätkretazische Extension von Ost nach West. Diese Extension wird deshalb als Folge der Instabilität eines westwärts vorstossenden Orogenkeiles interpretiert. Im Gegensatz dazu war die tertiäre Ost-West-Extension begleitet von Nord-Süd-Verkürzung.

Der Nachweis von zwei orogenen Zyklen widerspricht der klassischen Auffassung der alpinen Orogenese im Sinne einer kontinuierlichen tektonometamorphen Entwicklung von kretazischer Subduktion und Hochdruckmetamorphose zu tertiärer Exhumation und Barrow-Typ-Metamorphose. Vielmehr postulieren wir, dass es zweimal, in der Kreide und im Tertiär, zur Deckenstapelung im Zusammenhang mit Subduktion und zur nachfolgenden Exhumation, verbunden mit Extension, gekommen ist.

ABSTRACT

The structural analysis of the Austroalpine units in Graubünden reveals the existence of two orogenic cycles, Cretaceous and Tertiary in age, both including thrusting followed by extensional overprint. Such extensional

faulting occurred in the Late Cretaceous and in the Early to Mid-Oligocene. In both episodes, the direction of extension was parallel to the strike of the Alpine chain.

Five stages of the tectonic evolution are recognized: (1) Late Cretaceous nappe imbrication and sinistral transpression (Trupchun phase). The Austroalpine nappe pile was assembled by oblique east-over-west imbrication of the northwest margin of the Apulian microcontinent and was affected by sinistral transpression, localized in the east-west trending Albula steep zone. (2) Late Cretaceous extension (Ducan-Ela phase). The nappe pile was overprinted by top-east to top-southeast directed normal faulting. Recumbent folds developing simultaneously with and in the footwalls of large low-angle normal faults reflect east-west extension and vertical shortening of initially steeply oriented layers. Normal faulting and recumbent folding are therefore viewed as different expressions of the same extension process. (3) Early Tertiary collisional deformation (Blaisun phase). The Late Cretaceous extensional features were overprinted by east- to southeast-striking folds which are probably coeval with Early Tertiary northward thrusting of the entire Austroalpine nappe pile ("orogenic lid") over the deeper Penninic units. (4) Early to Mid-Oligocene extension (Turba phase). This second episode of east-west extension affected the boundary zone between the orogenic lid and the underlying Penninic units, locally leading to an extensional decoupling between these two levels (Turba mylonite zone). (5) Late Oligocene post-collisional shortening (Domleschg phase). The direction of shortening changed to NW-SE at this time.

On the scale of the entire Austroalpine realm, both Cretaceous shortening and following Late Cretaceous extension migrated westward. This first extensional event is therefore interpreted to be caused by instability of a westward advancing orogenic wedge. In contrast, Tertiary east-west extension was contemporaneous with ongoing north-south shortening.

The recognition of two orogenic cycles contradicts the classical view that the Alpine orogeny involves a continuous tectonometamorphic evolution from Cretaceous subduction and high-pressure metamorphism to Tertiary exhumation and Barrow-type metamorphism. Instead, it is postulated that nappe formation related to subduction and exhumation associated with extension occurred twice during the Alpine orogeny.

1 Introduction

Graubünden (SE Switzerland) is a key area for the reconstruction of the Alpine tectonic evolution. In this area, the Austroalpine nappes represent remnants of the southern continental margin of the Alpine Neotethys ocean. They overlie Penninic units, partly derived from oceanic crust, from the northern continental margin, and from continental fragments within the oceanic realm. In other parts of the Alps, the Austroalpine-Penninic contact can only be studied in isolated windows (e. g. Tauern window) or klippen, or has been overprinted by late postcollisional faults such as the Insubric line. The well-exposed, north-south trending Austroalpine-Penninic boundary in Graubünden, however, allows a correlation between the structures and deformational histories of all major units involved in the formation of the Alps. (For a comprehensive introduction into the regional geology and its problems, the reader is referred to Trümpy & Haccard 1969. A short overview is given in Trümpy 1980.)

Although an excellent data set on the regional geology and stratigraphy has been assembled by several generations of geologists, the structural architecture of the Austroalpine units in Graubünden is still poorly understood. This has several reasons. Firstly, Alpine deformation occurred under nonmetamorphic to greenschist facies conditions and affected lithologically heterogeneous units. Therefore the deformation is variable in style and intensity. Competent rock units like the Upper Triassic dolomite remained undeformed or were affected by brittle faults, while shaly formations took up large amounts of strain. As a result, the correlation of structures between different rock units or areas is difficult. Secondly, the Austroalpine nappe pile was formed by imbrication of a passive continental margin of Jurassic age. The crustal structure of this margin had already been strongly disturbed during the rifting phase. The interference of rift-related faults with Al-

pine thrust faults resulted in a complicated geometry of the nappe pile. Thirdly, this nappe pile was overprinted by several phases of post-nappe refolding and faulting, largely obscuring the original configuration. These complexities have resulted in long-lasting and vigorous controversies about the correlation of nappes, e. g. across the Engadine line (a major post-nappe fault), and about the directions of thrusting.

The direction of thrusting in the Austroalpine became controversial soon after the existence of large-scale thrusting in the Eastern Alps had been revealed by Termier (1903). Termier himself assumed a northwestward transport of the Austroalpine nappes (1903, p. 762). Rothpletz (1905), however, postulated west-directed thrusting (see Oberhauser 1991), which was rejected by most authors (e. g. Heim 1922, p. 867). Spitz & Dyhrenfurth (1913, 1914) also postulated west-directed thrusting based on the observation of westward-convex fold arcs in Graubünden, the "Rhätische Bögen". In contrast, Heim (1922, Fig. 227), Eugster (1923, Fig. 32) and Staub (1924, Fig. 34) arrived at a picture of overall east- to northeast-trending fold arrays by correlating folds in the Ela nappe with folds in the northwestern part of the Engadine Dolomites. They deduced north- to northwest directed thrusting. Recently, the view of Spitz and Dyhrenfurth and their predecessor Rothpletz has won new credit by structural and microstructural work on mylonites from thrust faults in the Eastern Alps in general (Ratschbacher 1986), and along the southwestern border of the Oetztal nappe in particular (Schmid & Haas 1989). These studies have shown that internal thrusting within the Austroalpine complex was in fact predominantly directed towards west. Strain analysis in the Arosa zone at the base of the Austroalpine indicated westward thrusting followed by northward thrusting (Ring et al. 1988, Ring et al. 1989). On the other hand, microstructural work also revealed that some of the faults and shear zones, which had previously been interpreted as thrusts, had the "wrong" sense of shear, i. e. top-east (e. g. Müller 1982), and do in fact represent low-angle extensional faults (Nievergelt et al. 1991 and in press, Werling 1992, Liniger 1992, Handy et al. 1993). Even some spectacular recumbent folds like the Ela "frontal fold" are not related to thrusting and crustal shortening, but to crustal extension (Froitzheim 1992).

Although these recent structural observations have largely improved the knowledge about the tectonic evolution of the Austroalpine, they have not yet been integrated into a general picture. The purpose of the present paper is therefore to define the temporal and spatial relations between the deformational structures of the Austroalpine units, and propose a structural evolution scheme that is not only locally valid, but applies to the whole area of the Austroalpine in Graubünden. Of course, the proposed scheme is only a first attempt towards a final synthesis. It will have to be tested and certainly modified in the future.

After a short overview of the Austroalpine nappes (chapter 2), the paper focuses on the area of the southwestern Silvretta, Ela and Err-Carungas nappes, serving as a "type area". There, structures of and overprinting relationships between different deformation phases are especially well preserved (chapter 3). As a base of our analysis of this area, we used the excellent regional studies and geological maps of earlier authors, in the Silvretta-Ela-Err area mainly those of Brauchli (1921), Brauchli & Glaser (1922), Eugster (1923, 1924), Ott (1925), Frei (1925), Frei & Ott (1926), Eggenberger (1926), Eugster & Frei (1927), Eugster & Leupold (1930), Cornelius (1932, 1935, 1950), Bearth et al. (1935), Stöcklin (1949) and Heierli (1955). The results of these authors had been complemented and in part corrected by stratigraphic-sedimentologic work of a research group led by

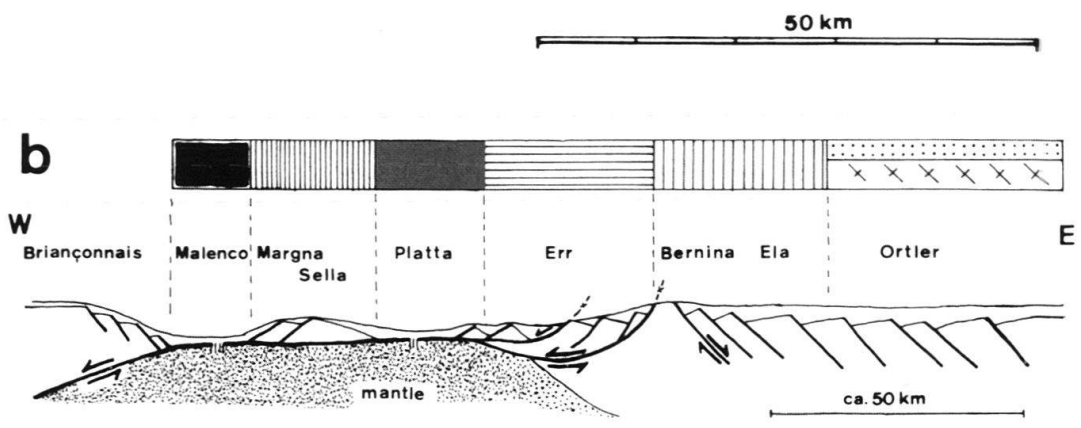
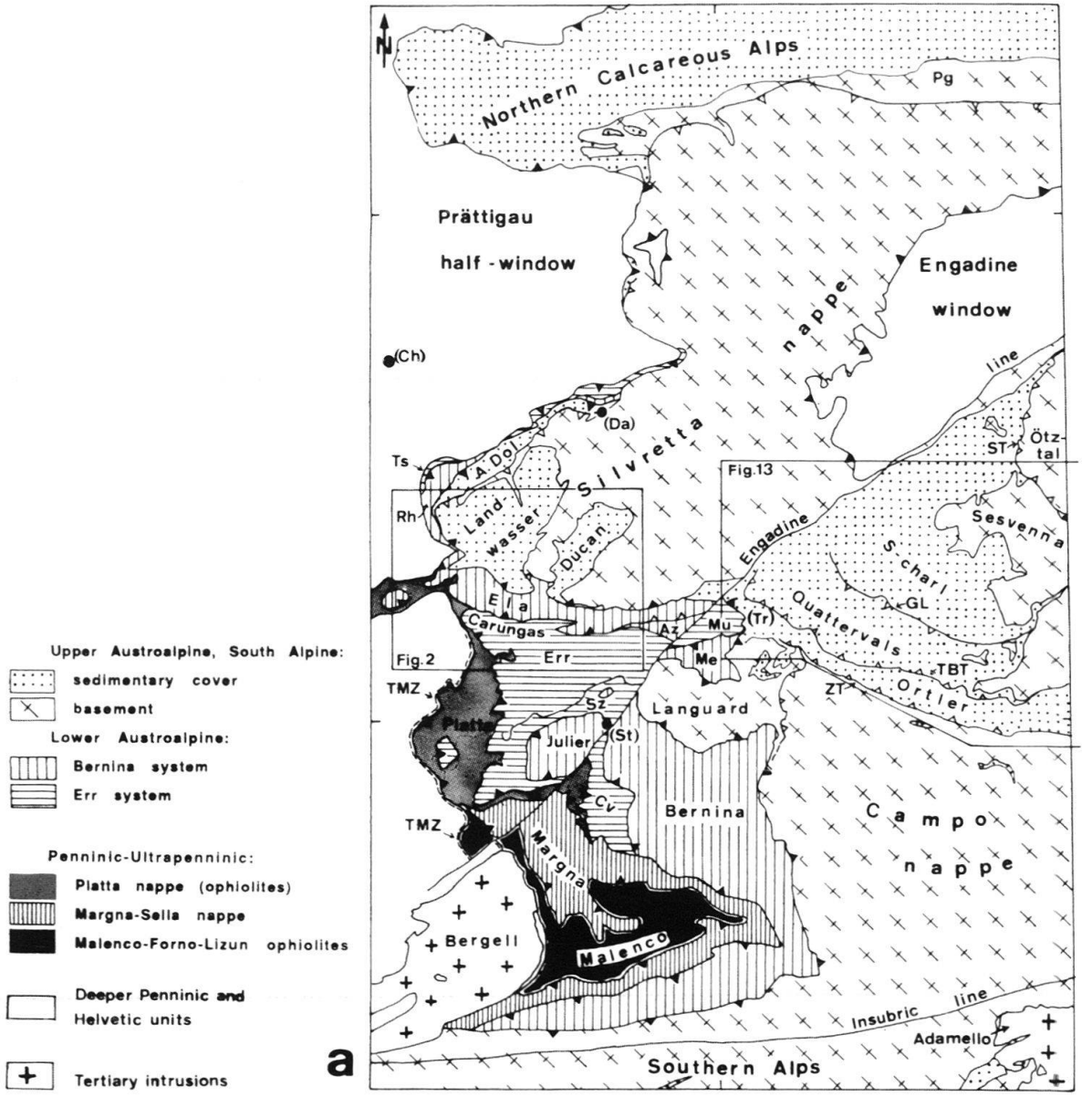
R. Trümpy (Furrer 1993, Eichenberger 1986, Naef 1987, Eberli 1985, 1988, and numerous diploma theses). All these studies provide a very detailed data set concerning the general geology of the area. Within this framework, we studied and mapped outcrop-scale deformation structures with an emphasis on structural overprinting. Direction and sense of displacement of major fault structures were determined by microstructural examination of mylonites and cataclasites.

Based on the structural analysis of the southwestern Silvretta, Ela and Err-Carungas nappes, a sequence of deformational phases will be developed and regional names will be introduced for these phases (chapter 4). In a next step the results from the Silvretta-Ela-Err region will be compared to and complemented with structural observations in the Engadine Dolomites (chapter 5). Finally, we will attempt a synthesis of the tectonic evolution of the Austroalpine units in Graubünden (chapter 6).

2 Austroalpine tectonic units in Graubünden and their position in the Jurassic passive continental margin

In this paragraph we give an overview of the Austroalpine nappe pile. Because the quantity of nappes and minor tectonic units must be confusing to readers not familiar with the area, a block diagram (P1.1) is attached, showing all the mentioned units and their mutual relations in a simplified way. The term “nappe”, as used in this paper, simply means a tectonic unit that is internally (more or less) coherent but completely separated from overlying, underlying and adjacent units by major Alpine (Cretaceous or Tertiary) faults.

The Austroalpine nappes resulted from tectonic imbrication of a passive margin of Jurassic to Early Cretaceous age, and the major tectonic units roughly correspond to paleogeographic domains of this margin (Fig. 1b; Froitzheim & Eberli 1990). The following major units or “nappe systems” can be distinguished in this way (Fig. 1, Pl. 1): (1) The Upper Austroalpine nappe system, also called Central Austroalpine (Trümpy 1980), represented by the Ötztal, Silvretta, Campo and Languard basement nappes, the Sesvenna – S-charl nappe (Sesvenna basement and its partly detached sedimentary cover in the S-charl unit of the northern Engadine dolomites), and completely detached sedimentary cover units like the Quattervals nappe, Ortler nappe and the Arosa Dolomites. These nappes were derived from the proximal, continentward part of the passive margin, characterized by east-dipping normal faults active in the Liassic (Furrer 1993, Eberli 1988, Froitzheim 1988, Conti et al. 1994). (2) The Bernina system, comprising the Bernina nappe s.l. with the exception of the Corvatsch and Sella units, further comprising the Mezzaun unit and the Corn slice, the Julier nappe and klippen of the Samedan zone (e. g. Piz Padella), most of the Albula zone, the Ela nappe and the Rothorn nappe (Rothorn basement and sedimentary cover). These units were derived from the “outer basement high” of the passive margin and from a number of basins east of this high which were bounded by east-dipping normal faults, active in the Liassic and a second time in the Middle Jurassic (Furrer 1993, Eberli 1988). (3) The Err system, comprising the Err-Carungas nappe, the Samedan zone with the exception of the klippen of Bernina nappe, the Corvatsch nappe, most of the Murtiröl unit and the Tschirpen nappe. This paleogeographic domain is characterized by one or more top-west directed extensional detachment faults (Froitzheim & Eberli 1990), overlain by tilt blocks, active in the Middle



Jurassic, and by the widespread occurrence of basement clasts in Middle to Upper Jurassic breccias. (4) The Platta nappe, including ophiolites and thin slivers of continental basement, Triassic and Jurassic sedimentary rocks in Austroalpine facies, representing an oceanic domain between the margin s. str. and the Margna-Sella continental fragment. (5) The Margna-Sella system, continental basement with a Mesozoic sedimentary cover in Austroalpine facies, derived from a continental fragment that became separated from the margin by extensional faulting in the Middle Jurassic. This fragment may have been connected to the Austroalpine farther south. (6) The Malenco-Forno-Lizun ophiolites of the South Penninic ocean.

All these units together form the "orogenic lid" (Laubscher 1983), a nappe pile that was assembled in the Cretaceous and that overrode the deeper Penninic units as a coherent thrust mass during the Early Tertiary. The lid includes not only Austroalpine units but also the South Penninic ophiolite units mentioned above (Liniger & Nievergelt 1990).

Bernina and Err systems are traditionally termed Lower Austroalpine. The Margna-Sella system may be referred to as "Ultrapenninic" following a suggestion by Trümpy (1992). Following Liniger (1992), we assume that the present position of the Platta ophiolites between the Lower Austroalpine above and the Margna-Sella system below does not result from Alpine backfolding or backthrusting but reflects the original paleogeographic arrangement of these units. The Ela nappe is Upper Austroalpine according to most authors (e. g. Spicher 1972) but belongs to the Lower Austroalpine Bernina system in our view (Schmid & Froitzheim 1993, see also chapter 5.2).

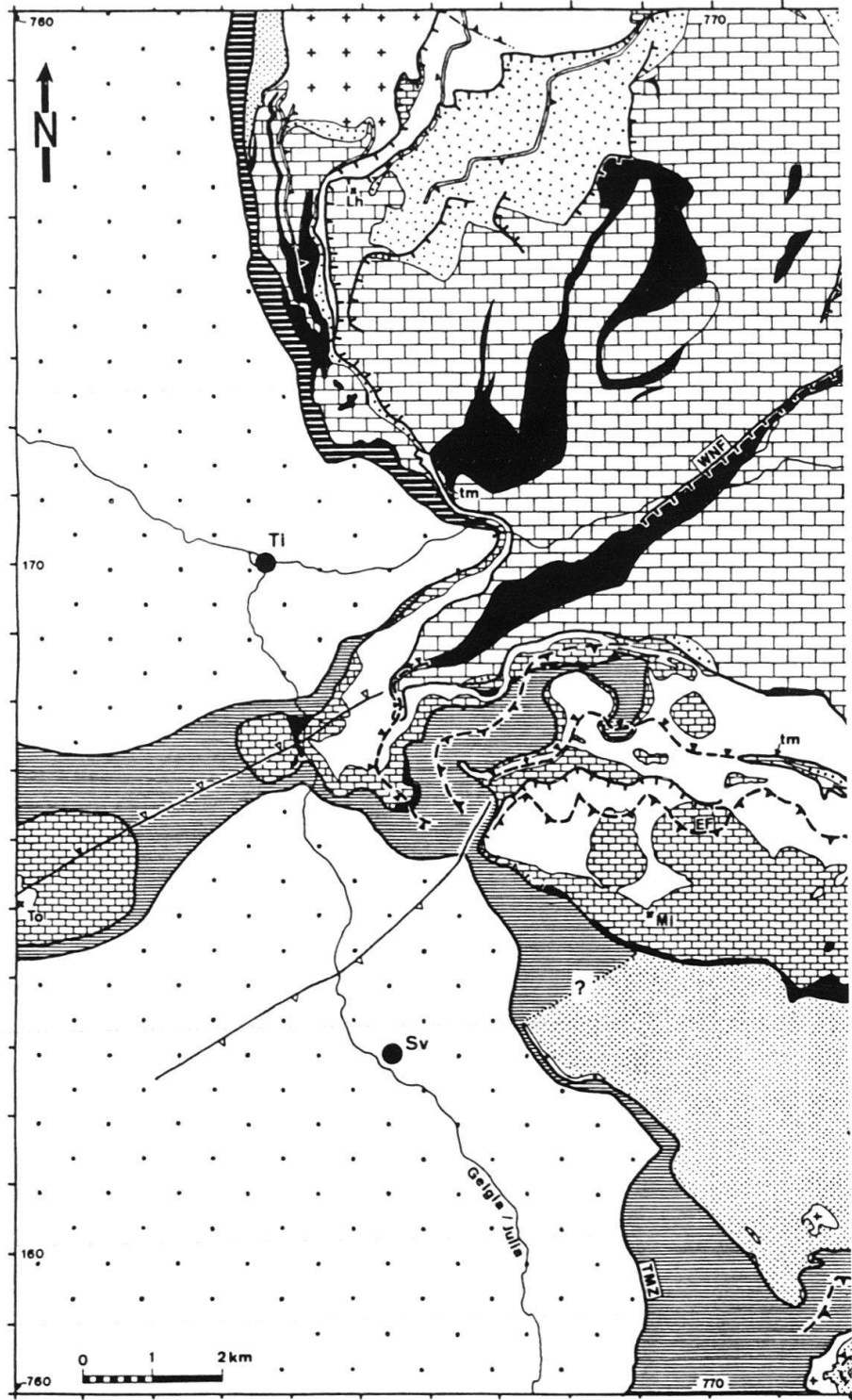
3 Alpine deformation of the southwestern Silvretta, Ela and Err-Carungas nappes

In the following, an area of the Austroalpine nappe edifice west of the Engadine line is described in detail (Fig. 2). The structural architecture of this area records the sequence of Alpine deformation events in a particularly clear way.

In this area, three major tectonic units of the Austroalpine are exposed (Figs. 1, 2): Silvretta nappe, Ela nappe and Err-Carungas nappe. The Silvretta nappe is a large Upper Austroalpine thrust sheet consisting predominantly of basement rocks, mostly gneiss and amphibolite. Cover rocks of Permian to Late Triassic age are only preserved at its southwestern edge in the Landwasser and Ducan synclinal areas (Fig. 1). Along its southern border, the Silvretta nappe is underlain by the Ela nappe, a detached and folded thrust sheet of Upper Triassic dolomite and Lower Jurassic to Cretaceous shale and limestone, lacking rocks older than Late Triassic. The Ela nappe is underlain by the Err-Carungas

Fig. 1. (a) Tectonic map of the Austroalpine and underlying upper Penninic nappes in Graubünden. Small triangles along tectonic boundaries point in the direction of the structurally higher unit, without indicating the nature of the boundary (some are not thrusts but low-angle normal faults). A Dol, Arosa dolomites; Cv, Corvatsch nappe; Me, Mezzaun unit; Mu, Murtiröl unit; Pg, Phyllitgneiss zone; Rh, Rothorn nappe; Sz, Samedan zone; Ts, Tschirpen nappe; GL, Gallo line; ST, Schling thrust; TBT, Trupchun-Braulio thrust; TMZ, Turba mylonite zone; ZT, Zebro thrust; (Ch), Chur; (Da), Davos; (St), St. Moritz; (Tr), Val Trupchun.

(b) Reconstructed east-west cross-section of the southeastern continental margin of the South Penninic ocean in the Late Jurassic and boundaries of the main Alpine tectonic units. Geometry of continent-ocean transition reconstructed assuming tectonic denudation of subcontinental mantle along top-west extensional detachment faults, according to model of Lemoine et al. (1987). For further explanation see text.



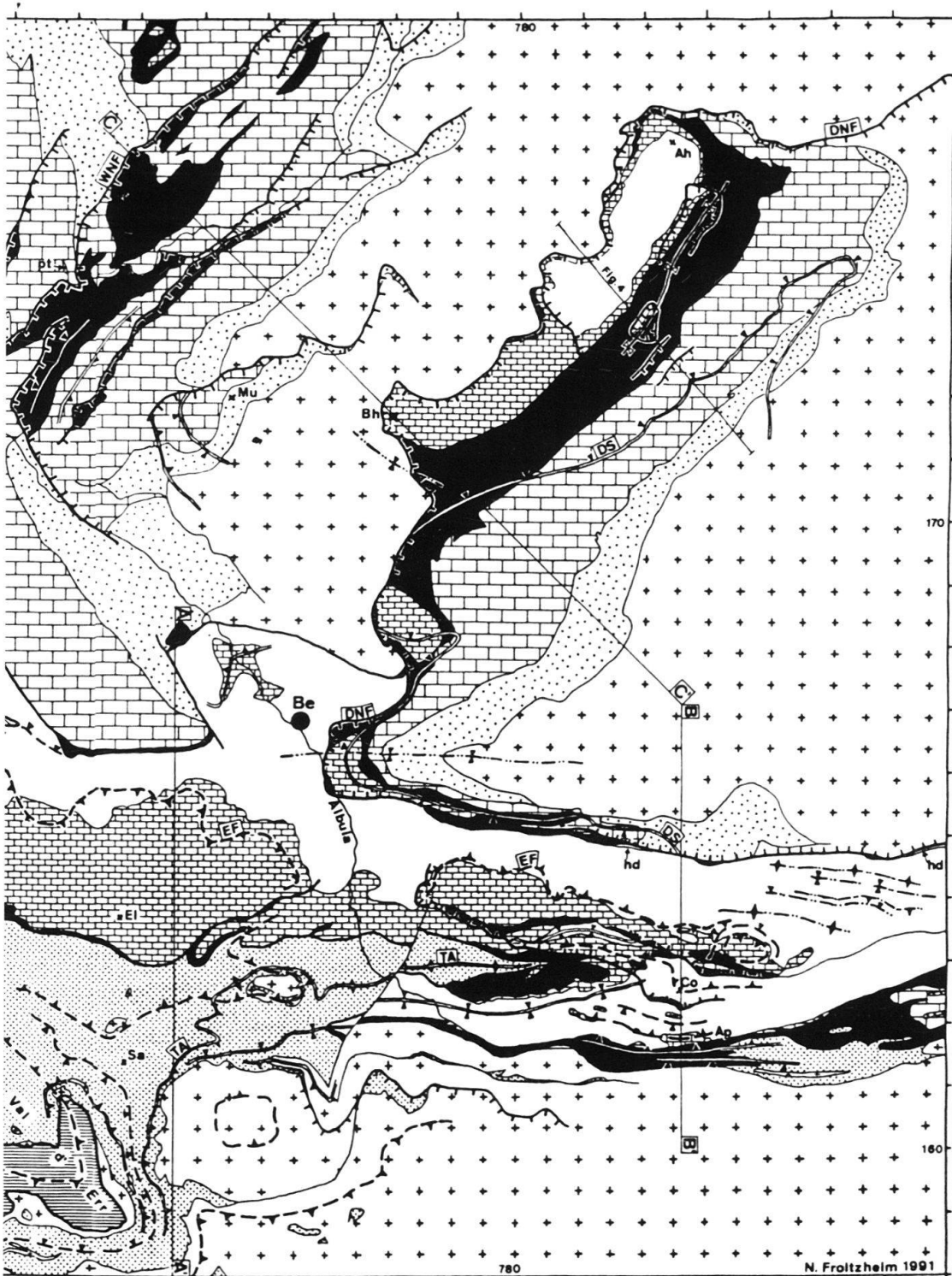
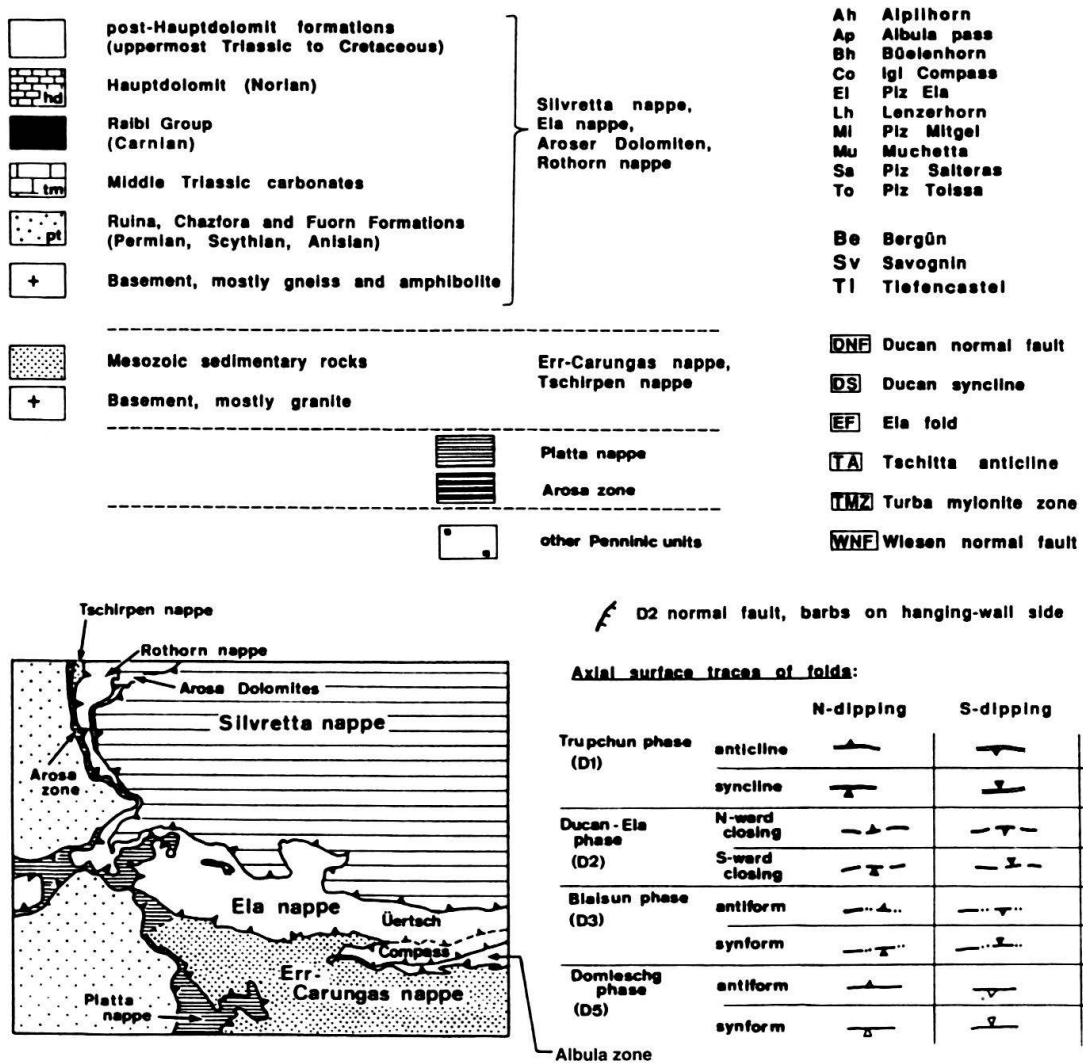


Fig. 2. Tectonic map of the southwestern Silvretta nappe, Ela nappe and northern Err-Carungas nappe. Geological base map compiled using maps of Brauchli & Glaser (1922), Frei & Ott (1926), Eugster & Frei (1927), Eugster & Leupold (1930), Cornelius (1932), Bearth et al. (1935), Stöcklin (1949), unpublished maps by D. Bollinger, M. Eberle, G. P. Eberli, U. Eichenberger, S. Frank, H. Furrer, T. Gronowski, H. Lozza, A. Rohrbach, M. Weh, D. Wurster and own mapping.



Legend for Fig. 2 (p. 566/567).

nappe, belonging to the Err system of the Lower Austroalpine nappes. This nappe includes pre-Mesozoic basement as well as a cover series of Permian to Cretaceous age.

East of the Albula pass, (southeastern corner of map, Fig. 2), an additional, minor unit is exposed between the Ela nappe above and the Err-Carungas nappe below, the Albula zone (Eggenberger 1926, Heierli 1955). This is a stack of thin, imbricated slivers comprising stratigraphic series from pre-Permian basement to Carnian evaporite, and occasionally also Jurassic and possibly Cretaceous strata (see Fig. 5a in Schmid & Froitzheim 1993). From the Albula pass towards the west, the Albula zone is only represented by a thin layer of Carnian carnageule at the base of the Ela nappe. Still further to the west, this layer becomes indiscernible from the basal carnageule of the Ela nappe.

Tectonic contacts between the three major thrust sheets (from top to bottom: Silvretta, Ela, Err-Carungas) are steeply north-dipping or subvertical (e. g. Fig. 3b). Hence this

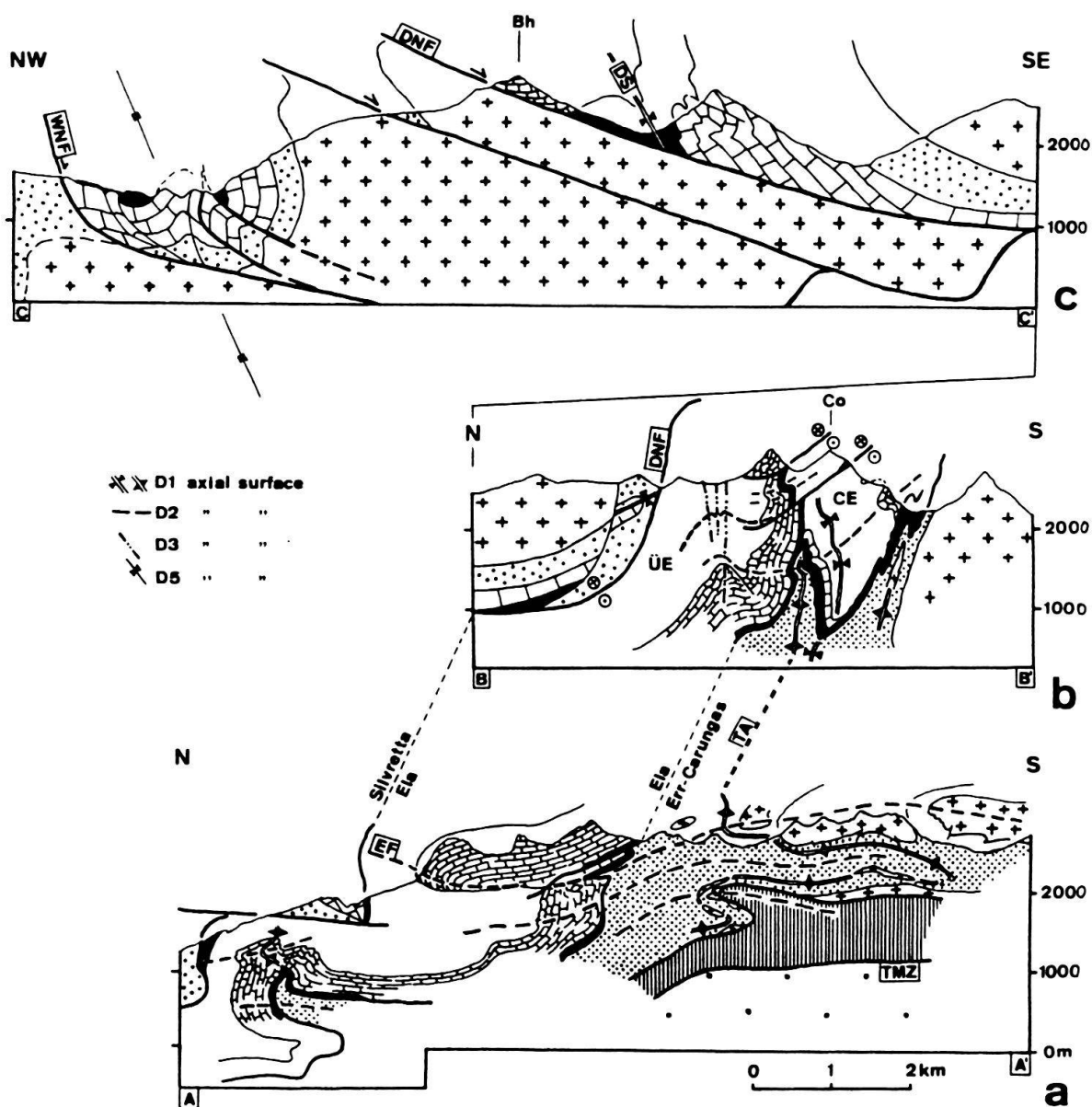


Fig. 3. Profiles from the Silvretta through the Ela into the northern Err-Carungas nappe. Profile traces and legend in Fig. 2. CE, Compass element, UE, Üertsch element of the Ela nappe.

stack of imbricates is now found side by side, with the highest unit to the north. Upper Penninic units appear under the Austroalpine in the western part of the map (Fig. 2): the Platta nappe to the south and the Arosa zone to the north. Both units comprise ophiolites derived from oceanic crust of the South Penninic ocean.

In the following, the structures observed in the three thrust sheets are described, proceeding from top (Silvretta nappe) to base (Err-Carungas nappe). A short general description precedes the structural analysis of each nappe.

3.1 Southwestern Silvretta nappe (Ducan area)

3.1.1 General description

The Ducan area of the Silvretta nappe (NE part of map, Fig. 2) is characterized by a Permian to Upper Triassic sedimentary cover series, preserved in a northeast-trending syncline (Ducan syncline). The syncline is bordered on both sides by pre-Mesozoic basement. The sedimentary sequence of the Ducan area comprises volcanoclastic and clastic Permian to Lower Triassic rocks, Middle Triassic dolomite and limestone, evaporite-bearing Raibl Group of Carnian age, Hauptdolomit (Norian), and Kössen Formation (Rhaetian), preserved in the core of the syncline (Eugster 1923, Eichenberger 1986). The syncline faces northwest. Its northwestern, normal limb is strongly attenuated or cut off by normal faults. The Mesozoic formations of this northwestern limb overlie the basement along a tectonic contact, the Ducan normal fault (Figs. 3c, 4). In contrast, the southeastern, vertical to overturned limb is well preserved, only cut by minor normal faults. The transgressive contact of Permian on basement is still preserved in this limb.

At the southwestern termination of the Ducan syncline, the Permo-Mesozoic fill of the syncline directly rests on the Ela nappe, and the Silvretta basement is omitted. West

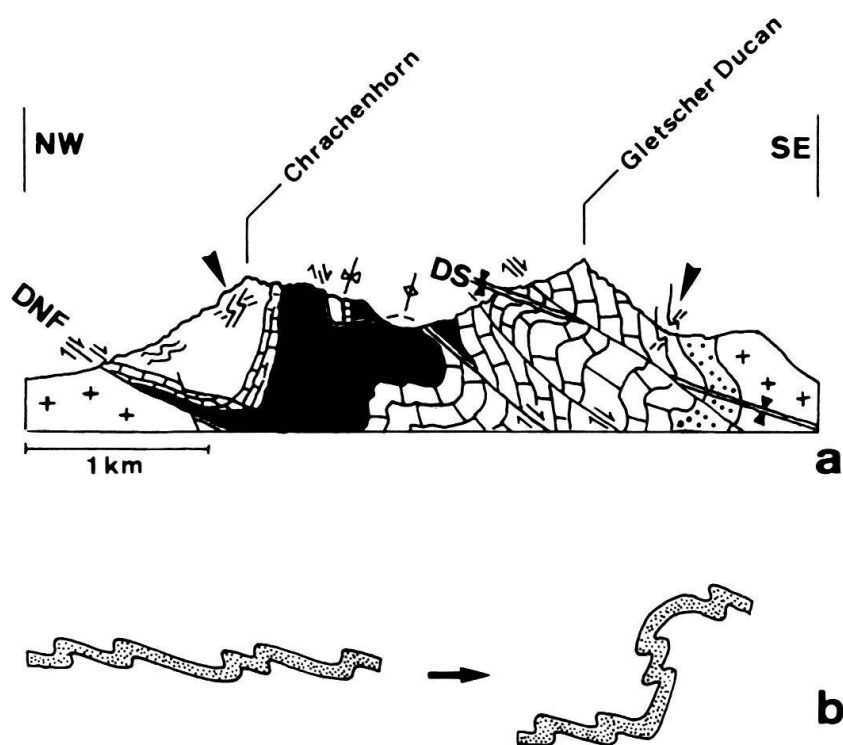


Fig. 4. (a) Cross-section of the central part of the Ducan syncline, after Eichenberger (1986), Wurster (1991) and own observations (trace of section in Fig. 2, same legend same as Fig. 2). DS, axial trace of D₁ Ducan syncline, DNF, Ducan normal fault. Solid arrows indicate minor folds with "wrong" vergence relative to large-scale folds. Southeast-dipping normal faults, including the Ducan normal fault, crosscut the D₁ folds. The syncline-anticline pair in the middle of the section, deforming the normal fault, is tentatively correlated with late NE-striking folds (Domleschg phase).

(b) Explanation for vergence of D₁ folds: Minor folds were slightly earlier formed and subsequently rotated during formation of large scale folds. This is interpreted as two stages in a continuous process.

and East of the Ducan syncline, however, the Silvretta basement reappears. This peculiar situation was interpreted by Trümpy (1980, p. 80) in the following way: the Silvretta nappe was first folded (Ducan syncline, Landwasser syncline) and then detached and transported westward along a thrust which truncated the base of the two synclines. As we will show below, we arrive at a slightly different picture: the southwestern Silvretta nappe shows the imprints of early thrusting and folding followed by normal faulting. Finally, the normal faults were deformed in a second folding event.

3.1.2 D_1 folding and thrusting in the Silvretta nappe

Minor folds with amplitudes of 10 to 100 metres are observed in the Ducan syncline (Fig. 4 and profiles in Eugster 1923, Eichenberger 1986, Furrer et al. 1992). The folds have northeast- to north-trending axes and generally face northwest to west. They are associated with an axial plane cleavage in limestones and shales of the Middle and Upper Triassic, representing the oldest penetrative deformational structure in the sedimentary rocks of the Ducan area. Most of the minor folds can be interpreted as parasitic folds of the Ducan syncline. However, in at least two localities the folds have the wrong vergence in respect to their position in the syncline (folds indicated by thick arrows in Fig. 4a). The enveloping surfaces of the folds in these localities are vertical to overturned, that is, southeast-dipping. The axial surfaces of the folds dip northwest, and the facing direction is downward and northwest. In the absence of superposition criteria, these folds can be interpreted as originally northwest-vergent folds that were subsequently rotated anti-clockwise, looking northeast, when the large-scale Ducan syncline developed into its final shape (Fig. 4b). This is supported by the observation that “wrong-vergence” folds are restricted to steep to overturned limbs of the major folds. Although this interpretation implies a slightly older age for these minor folds in respect to the Ducan syncline, it is assumed that both were generated during the same process of west- to northwest directed shearing deformation (D_1).

Towards the southwestern termination of the Ducan syncline, the strike of minor D_1 folds changes from northeast to north and eventually northwest (Spitz & Dyhrenfurth 1913). The same is true for the hinge of the Ducan syncline which thus describes a westward-convex arc, one of the “Rhaetic arcs” of Spitz & Dyhrenfurth (1913). Therefore, sedimentary rocks of the Ducan syncline can be followed towards the east and along the base of the Silvretta nappe into the area north of Albula pass (Fig. 2). The bending of the fold axes is not smooth but associated with intense brittle deformation (Eugster 1923, p. 101).

A northwest- to west-trending stretching lineation was found in strongly sheared Permian to Lower Triassic sandstones and conglomerates of the Ducan syncline in Val Tisch (coord. 782.8/164.7) and in the Landwasser area, northwest of the Ducan syncline (coord. 767.35/177.05). This lineation is interpreted to approximate the shearing direction during D_1 folding. Hence, D_1 folding is related to the west- to northwestward directed transport of the Silvretta nappe.

3.1.3 D_2 normal faulting in the Silvretta nappe

The Ducan area, like the southwestern Silvretta nappe in general, is cut by numerous southwest- to south-striking, southeast- to east-dipping faults. Offset of marker horizons

generally indicates southeast-directed normal fault movement (Figs. 3c, 4). The most important of these faults is the Ducan normal fault or “Ducan-Scherfläche” of Eugster (1923), forming the northwestern boundary of the sedimentary rocks of the Ducan syncline. The Ducan normal fault cuts obliquely through the Ducan syncline, as can be seen in map view (Fig. 2) from the truncation of the axial trace of the syncline (DS) by the Ducan normal fault (DNF) northeast of Bergün. This relation indicates that the normal fault overprints and therefore postdates the Ducan syncline. This is confirmed by small-scale overprinting relations, like normal-fault-related drag folds deforming the D_1 cleavage (Wurster 1991).

Geometric relations along the southern continuation of the Ducan normal fault indicate that normal faulting not only postdates D_1 folding but also the emplacement of the Silvretta nappe on top of the Ela nappe. At a triple point 2 km northeast of Bergün, the Ducan normal fault truncates the basal thrust of the Silvretta nappe (small insert map in Fig. 5, see also Fig. 2). The contour lines of both faults in Figure 5 show that the normal fault (“A”) does not change its orientation at this triple point and that the Silvretta basal thrust (“B”) ends abruptly against the normal fault. South of the triple point, the Ducan normal fault changes its orientation from a southeastward dip into a steep northward dip, thus outlining an eastward-plunging synform (D_3 fold, see below). Further towards east, the Ducan normal fault continues in a north-dipping orientation along the base of the Silvretta nappe. This tectonic boundary (“C”) is interpreted as representing the Silvretta basal thrust, reactivated by the Ducan normal fault. According to this interpretation, the Ducan normal fault formed as an east-dipping, listric fault with a steeper upper segment that cut through the Silvretta nappe, and a lower, shallowly dipping segment that followed the basal thrust of the nappe. The part of the Silvretta nappe located in the hanging wall of the Ducan normal fault slipped back towards east. Thereby the sediments of the Ducan syncline were downthrown directly onto the Ela nappe and the Silvretta basement was omitted.

3.1.4 Fault rocks from the Ducan normal fault and the base of the Silvretta nappe

In order to test the hypothesis outlined above, namely that the Ducan fault represents a top-east to -southeast directed normal fault which partly reactivated the basal thrust of the Silvretta nappe, we investigated microstructures in fault rocks along the Ducan normal fault at Büelenhorn and along the Silvretta-Ela boundary north and northeast of Albulapass.

On the west side of Büelenhorn (Fig. 3c), the hanging wall of the Ducan normal fault consists of Upper Triassic Hauptdolomit and the footwall of pre-Permian orthogneiss (“younger orthogneiss”, Maggetti & Flisch 1993). Along the contact between dolomite above and gneiss below, a thin layer of strongly sheared fault rocks is exposed. The lower part of this, 40 cm thick, is cataclasite derived from Permian to Lower Triassic clastic rocks. The upper part, 1 to 2 meters thick, is intensely sheared limestone (Middle Triassic S-charl Formation). The preservation of a normal, although extremely thinned stratigraphic sequence suggests that deformation was ductile on the scale of the fault zone.

The fault rock shown in Figure 6a, derived from limestone of the S-charl formation, has an irregular, anastomosing foliation oriented roughly parallel to the shear zone boundaries. It exhibits a weak, east-southeast trending slickenside lineation. The plane of the

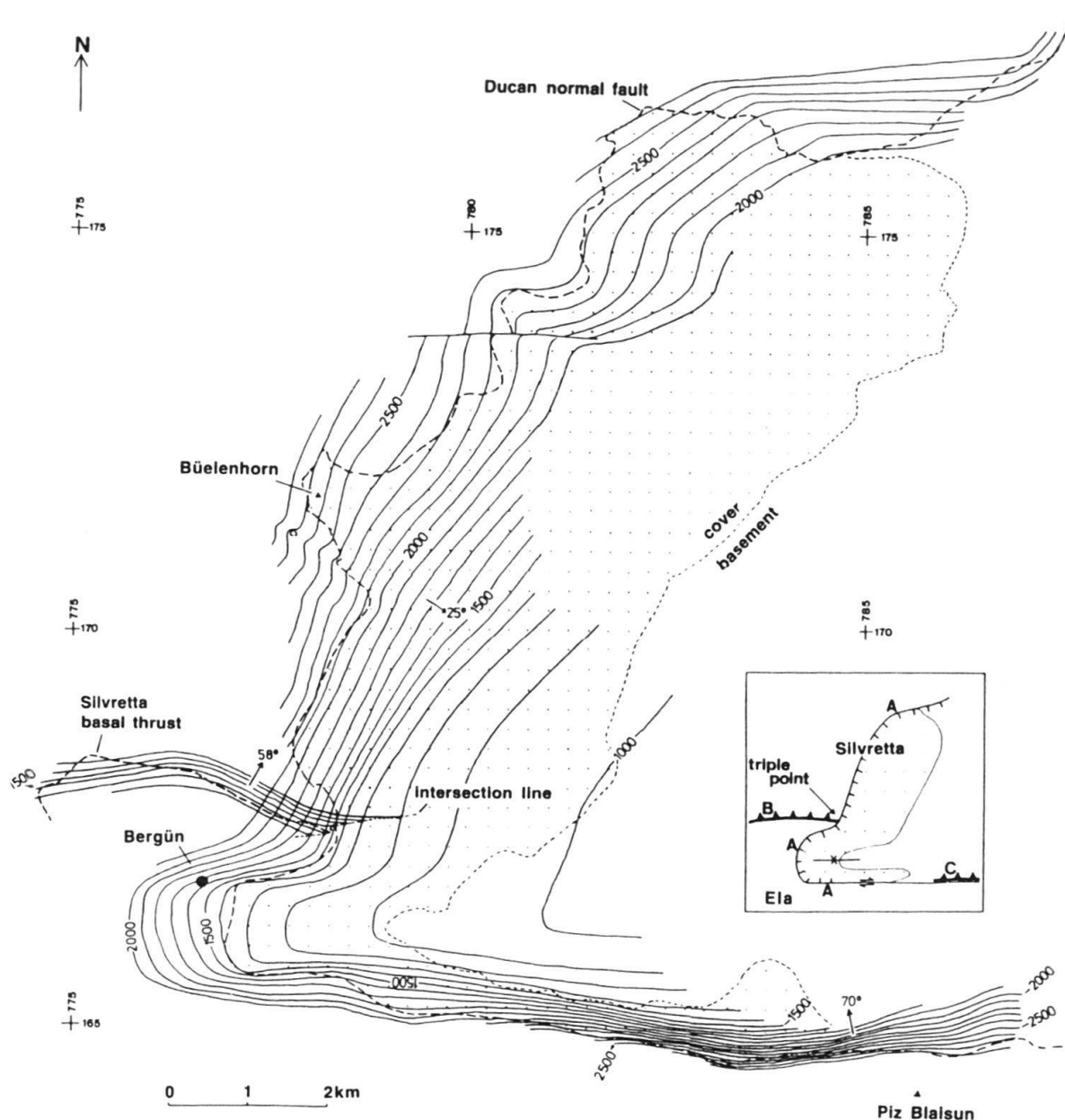


Fig. 5. Contour map of the Ducan normal fault (small insert map: A) and the basal thrust of the Silvretta nappe (B). (C) is the basal thrust, reactivated by the Ducan normal fault. Note truncation of the Silvretta basal thrust by the Ducan normal fault at triple point, and folding of the Ducan normal fault around an east-striking D_3 fold. Numbers along contour lines indicate elevation in metres above sea level, arrows with numbers indicate dip direction and angle of tectonic boundaries.

section is perpendicular to the foliation and parallel to the slickenside lineation. Stylolites and calcite veins are abundant in this rock. Two types of veins can be distinguished: first, extension veins filled with calcite crystals showing no signs of deformation (v_1), and second, calcite veins strongly overprinted by cataclastic shearing (v_2). The unsheared veins of the first type are generally at high angles to the fault-zone boundaries, whereas most of the sheared veins are at lower angles to the fault-zone boundaries. The stylolites are

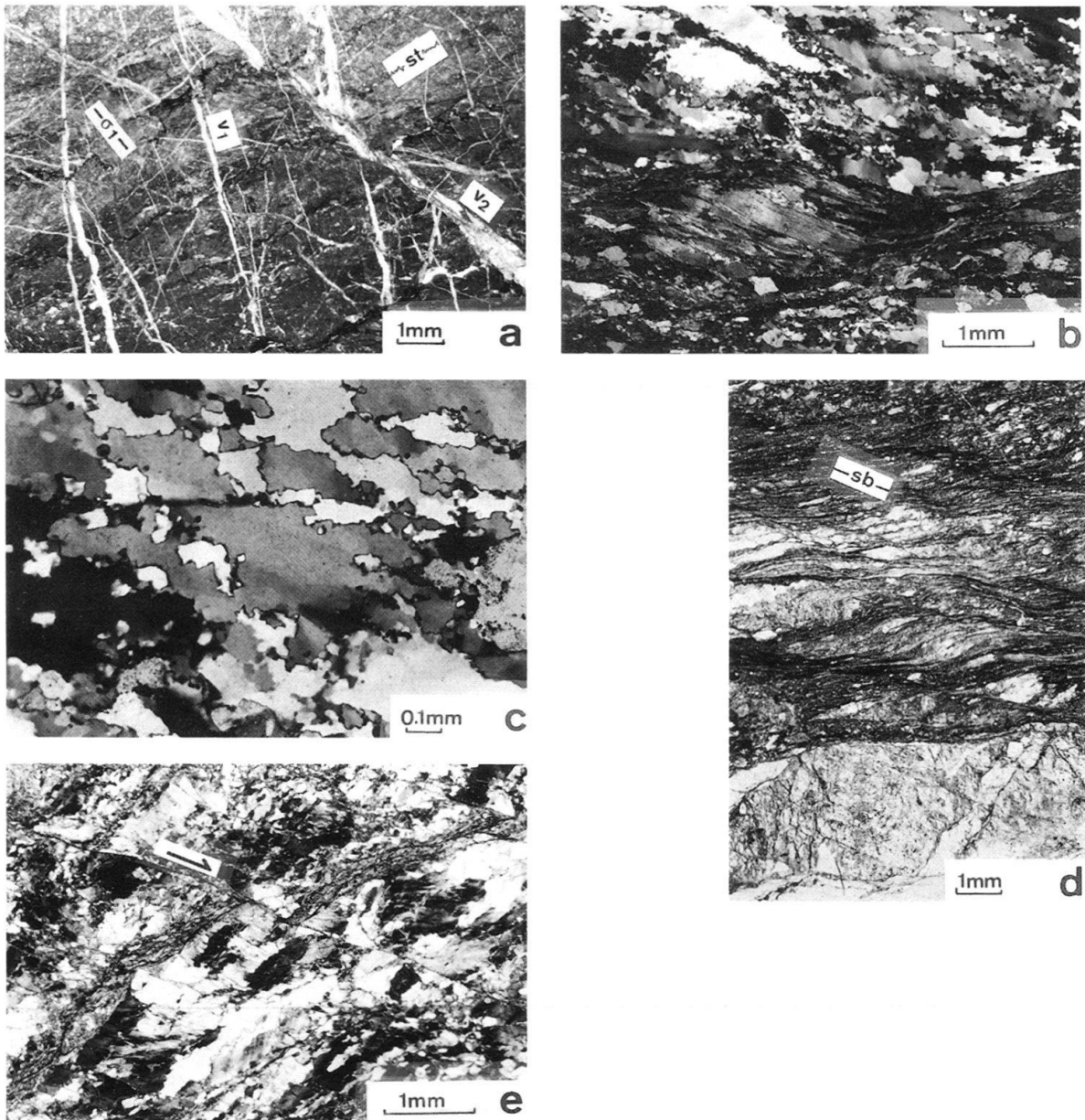


Fig. 6. Thin section micrographs of fault rocks from the Ducan normal fault and the base of the Silvretta nappe. In all micrographs, west is to the left and the fault-zone boundaries are horizontal.

(a) Cataclastic fault rock of the Ducan normal fault, showing stylolites (st) and two sets of veins, one with undeformed calcite filling (v_1), the other including dark zones of cataclastically sheared calcite (v_2). The two sets are interpreted as conjugate microfaults. Conjugate microfaults and stylolites indicate orientation of σ_1 as shown, compatible with dextral shear sense. Protolith is Middle Triassic limestone. West side of Büelenhorn (coord. 777.9/171.6).

(b) Mylonite from the base of the Silvretta nappe (first type, see text) formed from a gneissic protolith. Large muscovite "mica fish" (lower left) indicates sinistral (top-west) shearing. Northwest of Piz Belvoir (coord. 789.7/165.55).

(c) Quartz microstructure from same sample as in (b). Grain boundary migration led to preferred grain boundary orientations parallel to the foliation plane (horizontal) and at a high angle to the foliation plane (inclined to the right), indicating sinistral (top-west) shearing.

(d) Mylonitic to cataclastic fault rock from the base of the Silvretta nappe (second type, see text). Shear bands (sb) indicate dextral (top-east) shearing. Cinuos-chel (coord. 798.05/168.85).

(e) Same sample as in (d). Brittle, synthetic Riedel shear offsetting quartz grains in a dextral (top-east) sense.

roughly perpendicular to the bisecting plane of the acute angle included by the two sets of veins. Where the sheared veins offset other veins, the offset is top-east-directed.

Mutual crosscutting relations between veins of the two sets and stylolites (Fig. 6a) indicate that all these structures originate from the same deformation process. It is therefore assumed that the deformation of the fault rock included fracturing events intermittent with periods of pressure solution creep. During the fracturing events, the two sets of fractures formed as conjugate microfaults in response to stresses associated with fault slip. In the periods of pressure solution creep, calcite was dissolved along the stylolites and deposited in the fractures which opened up to form veins. The veins of the synthetic set (v_2) were again cataclastically sheared in a subsequent fracturing event. The angular relation between fault-zone boundaries, stylolitic seams, and veins indicates a top-east-south-east shear sense.

The microstructural study of cataclasites from the northwestern part of the Ducan normal fault thus confirms that the sedimentary rocks of the hanging wall were down-thrown towards east-southeast, that is, parallel to the dip of the fault, onto the gneiss of the footwall. Mylonites from the base of the Silvretta nappe along the presumed eastward continuation of the Ducan normal fault will be described next.

Between Fuorcla Pischa north of Albula pass and Cinuos-chel in the Upper Engadine valley, the Silvretta nappe is formed by ortho- and paragneiss. The amphibolite-facies metamorphism of these rocks is of Variscan age (370–350 Ma, Maggetti & Flisch 1993). They overlie Jurassic and Cretaceous sediments of the Ela nappe. Thin slivers of Triassic dolomite and cagneule occur in between (“Subsilvrettide Linsen”, Fig. 7, Heierli 1955). Mylonites with a clear foliation and stretching lineation, derived from gneissic protoliths, occur along the base of the Silvretta nappe. The mylonites have a thickness of a few metres to several tens of metres. They can be distinguished from the amphibolite-facies pre-Alpine gneisses by their lower-temperature, greenschist-facies overprint. The foliation of the mylonites dips towards north at different angles, mostly between 30° and 50° , parallel to the base of the Silvretta nappe, and the stretching lineation trends east to southeast. Two types of mylonites were observed within the same fault zone, characterized by a distinctly different deformational behaviour of quartz. Figures 6b and c represent the first type of mylonite. Crystal plastic flow in quartz aggregates is accommodated by extensive and pervasive syntectonic recrystallization. Both subgrain rotation and grain boundary migration recrystallization are observed, the latter mechanism leading to preferred grain boundary orientations parallel and at a high angle to the foliation plane (Fig. 6c). Mica fish (Fig. 6b), asymmetric porphyroclasts, shear bands, grain boundary preferred orientation, and crystallographic preferred orientation indicate a top-west to top-northwest sense of shear for these mylonites. A coaxial component of the deformation is indicated by sets of conjugate shear bands with opposite sense of displacement.

The second type of mylonite (Fig. 6d, e) has microstructures indicative of distinctly lower temperatures. In these mylonites, recrystallization of quartz is restricted to narrow bands. Outside of these bands, old quartz grains exhibit undulous extinction and contain deformation lamellae; often they are fractured. Cataclastic shear fractures are common (Fig. 6e). Crystallographic preferred orientation in a narrow recrystallized quartz band, grain shape preferred orientation, asymmetric porphyroclasts, pressure shadows and shear bands (Fig. 6d) indicate a top-east to -southeast movement. The mylonites of this second type obviously formed near the frictional-viscous transition (Schmid & Handy

1991) and overprinted the dynamically recovered and recrystallized mylonites of the first type.

The mylonites which formed at higher temperatures, indicating top-west to top-north-west shear, are interpreted to be related to initial detachment and thrusting of the Silvretta nappe. The younger, lower-temperature, top-east mylonites to cataclasites are interpreted as resulting from back-slipping of the Silvretta nappe towards east, along the original thrust. This surface acted as a prolongation of the Ducan normal fault towards the east and towards greater depth.

3.1.5 D₃ folding in the Silvretta nappe

The contours of the Ducan normal fault in Figure 5 outline an east-trending, open synform with an axis south of Bergün. Other, more gentle east- to southeast trending folds affecting the Ducan normal fault are outlined further north. These folds represent a second folding phase in the Silvretta nappe, associated with the third regional deformation event (D₃). A steeply dipping, west-northwest striking cleavage in sandstones and conglomerates of the Chazfora and Fuorn Formations at the base of the Ducan sedimentary sequence can be ascribed to this folding phase. These clastic sediments are often devoid of a cleavage related to D₁ folding so that the D₃ cleavage is the oldest penetrative structure observed. This cleavage is almost perpendicular to the axes of D₁ folds. D₃ cleavage also overprints Fuorn-Formation-derived cataclasites along the Ducan normal fault at Büelenhorn. This gives additional evidence for a post-normal-faulting (post-D₂) age of these folds.

In summary, we can distinguish three deformation phases in the southwestern Silvretta nappe, of which the first includes top-west to top-northwest thrusting and related folding around northeast-striking axes, the second, top-east-southeast normal faulting and the third, additional shortening accommodated by east- to southeast-striking folds. We arrive at an explanation for the relationship between Silvretta basal thrust and Ducan syncline that is different from the one of Trümpy (1980): in our view, the Ducan syncline was not formed before the detachment and thrusting of the Silvretta nappe, but during this process. It is true that the Ducan syncline is truncated in the southwest by the basal surface of the Silvretta nappe. This basal surface, however, does not represent the original thrust but rather a segment of the D₂ Ducan normal fault.

3.2 *Ela nappe*

3.2.1 General description

The Ela nappe is a detached and intensely folded sedimentary sequence. It underlies the Silvretta nappe to the south. The Carnian Raibl Group (dolomite, shale, sandstone and evaporite-derived cargneule) forms the décollement horizon at the base of the nappe. Norian Hauptdolomit is the relatively competent “backbone” of the nappe, whereas Rhaetian Kössen Formation and Lower to Middle Jurassic Allgäu Formation are dominated by shales, marls and limestones which generally are strongly folded. Thus the rocks of the Allgäu Formation are particularly well suited for structural analysis. Upper Jurassic and Cretaceous formations, including radiolarian chert, *Aptychus* limestone and Palombini shale, occur in the topmost parts of the nappe, immediately below the base of the

Silvretta nappe. They are separated from the latter by thin lenses of Triassic rocks, referred to as “Subsilvrettide Linsen” earlier. We subdivide the Ela nappe into an upper unit (Üertsch element) and a lower unit (Compass element, see Fig. 2, small map). The Compass element includes the “Gualdauna-Schuppe” as defined by Heierli (1955) and Eberli (1985) and the overlying Allgäu Formation of Igl Compass (Fig. 2, coord. 782.7/162.6). We chose such a subdivision because a major thrust surface is located between the Allgäu Formation of Igl Compass and the overlying Triassic dolomite of Piz Üertsch. This thrust was in part overprinted by low-angle normal faulting (see below).

In the northwestern part of the map (Fig. 2), the thickness of the Ela nappe decreases until it is represented by only a few metres of limestone in the (recently destroyed) outcrop at Belfort near Tiefencastel (Fig. 2; coord. 765.9/171.1; Trümpy 1980, p. 237). The geometric relations in this area, although badly exposed, suggest that the Ela nappe is continuous with the Rothorn nappe (“Rothornschuppe”, Brauchli 1921) exposed in the northwestern corner of the map area (Fig. 2). The latter comprises a gneissic basement and its Triassic cover.

Three generations of folds can be distinguished in the Allgäu Formation of the Ela nappe between Bergün and the Albula pass. All three are observed on different scales, from thin-section to cross-sectional view of the nappe (Fig. 3b).

3.2.2 D_1 folding and thrusting in the Ela nappe

Early folds in the Allgäu Formation of the Ela nappe are tight to isoclinal and associated with a well-developed axial plane cleavage and a mostly east-west trending lineation. This lineation is a cleavage-bedding intersection lineation but at the same time a stretching lineation as indicated by deformed markers, such as conglomerate pebbles and belemnite rostra. In contrast to the Silvretta nappe, lineation and cleavage are ubiquitous throughout the Ela nappe. Fold hinges are rarely found but always oriented parallel to the lineation. In general, they strike about east-west and gently plunge towards east or west (Fig. 7a). The facing of D_1 folds is generally towards south in those parts of the Ela nappe where the stratigraphic succession is in an overall upright position. Curving D_1 fold hinges or sheath folds have not been observed in the Ela nappe, in contrast to the underlying Err-Carungas nappe where they are common (see below).

The strong overprinting of D_1 folds by younger structures, most importantly recumbent D_2 folds, makes it difficult to reconstruct the large-scale geometry of D_1 . Nevertheless a reconstruction is attempted in Figure 8. Even after retro-deformation of D_2 folds, a two-stage evolution of D_1 structures needs to be proposed in order to explain the geometric relations. We assume that the south-facing folds (see above) were formed in an early stage of D_1 (Fig. 8a). In the Ela nappe, such south-facing D_1 folds are restricted to outcrop-scale structures and are only found in the Allgäu Formation. However, large south-facing D_1 folds with basement in the anticlinal cores and sediments in synclines are found in the southern part of the Rothorn nappe (NW corner of map, Fig. 2, coord. 764/176), the presumable northwestern continuation of the Ela nappe. These were already described by Brauchli (1921). The Üertsch element of the Ela nappe can be viewed as a south-facing, isoclinal syncline with a thick normal limb and an extremely thinned inverse limb, represented by the “Subsilvrettide Linsen”. (According to Heierli 1955 and Pittet 1993, these slivers include inverse-lying stratigraphic sequences.) The internal

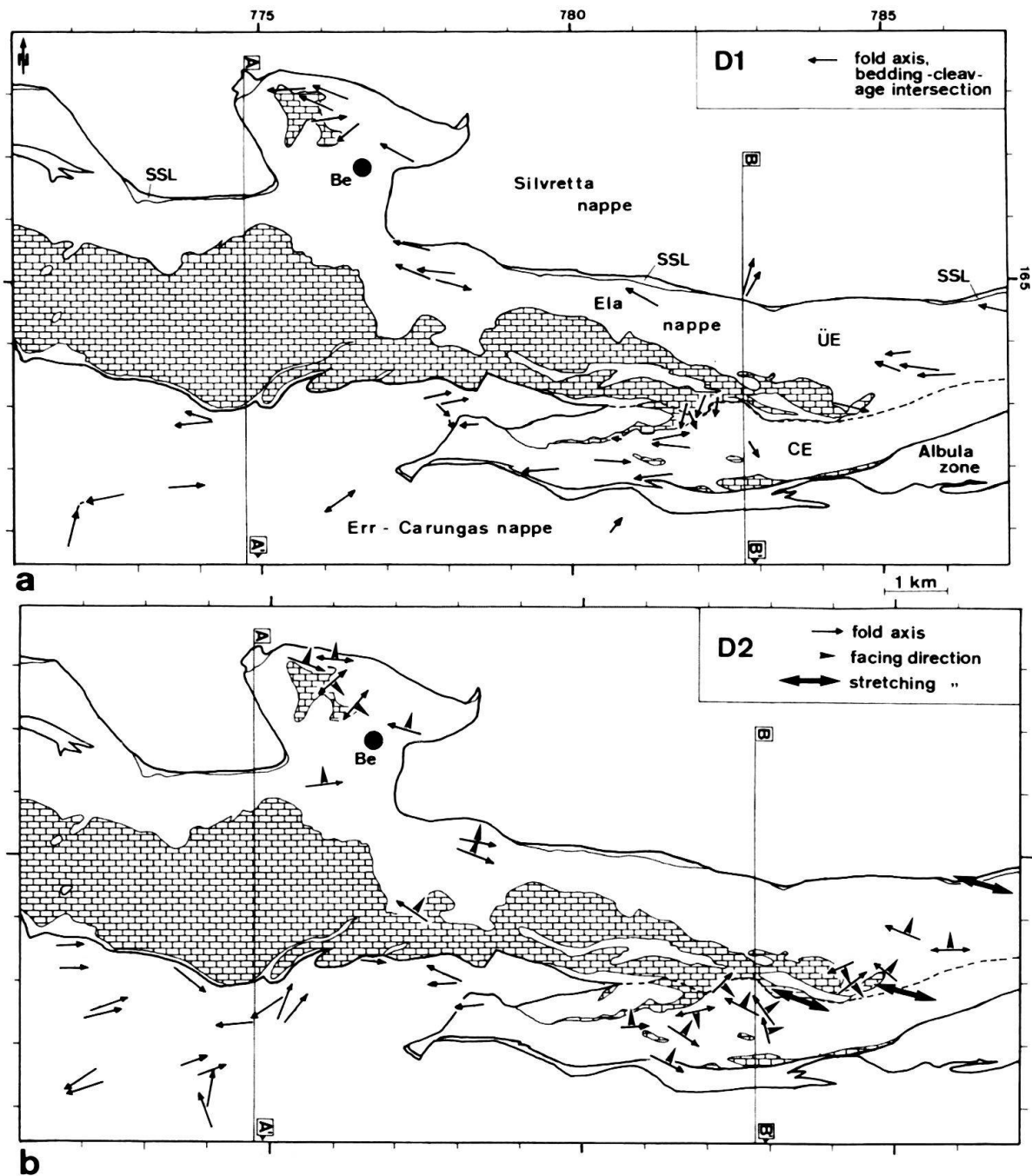


Fig. 7. Orientations of D_1 and D_2 fold axes in the Ela and northern Err-Carungas nappes. Arrows indicate plunge direction of fold axes, length of arrow correlates to plunge angle (longest arrows for horizontal fold axes, shortest arrows for subvertical fold axes). Be, Bergün; CE, Compass element; SSL, "Subsilvrettide Linsen"; ÜE, Üertsch element; brick signature for Hauptdolomit of the Ela nappe; traces of cross sections of Fig. 3 are indicated; other localities can be identified by comparison with Fig. 2.

(a) D_1 folds. Note that these trend northeast in the Silvretta nappe and in the Err-Carungas nappe, and that the Ela nappe represents a "channel" of east-west-trending D_1 folds between the two other nappes. Only in the basal part of the Allgäu Formation of the Ela nappe, near the underlying Hauptdolomit, more north-south trending D_1 folds occur.

(b) D_2 folds. Arrows without shaft indicate facing directions of F_2 folds. Facing is either towards north or south for east-west-trending folds, and generally towards northeast to southeast for more north-south-trending folds. Thick arrows with two heads indicate stretching directions in metre-scale extensional shear zones in the Allgäu Formation.

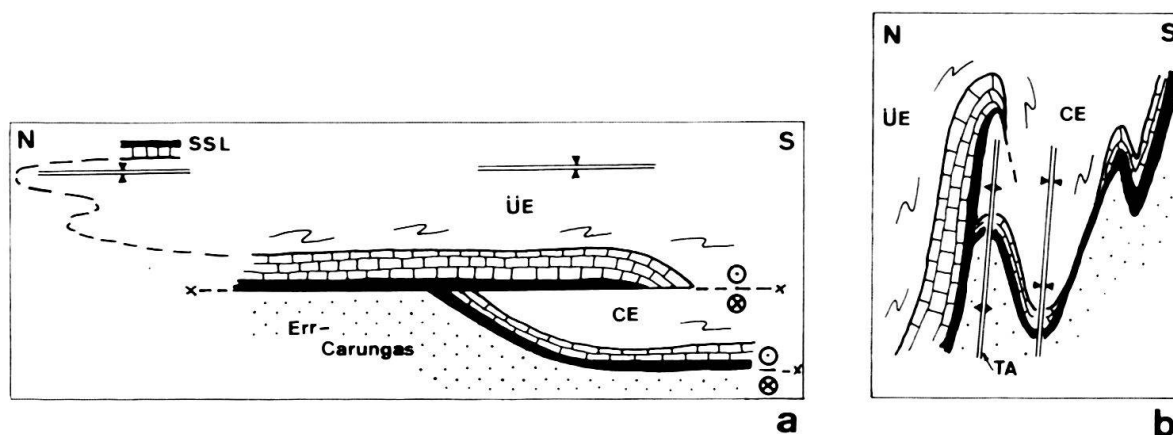


Fig. 8. Diagrammatic cross sections showing evolution of D_1 structures in the Ela nappe along profile of Fig. 3b. Legend of lithologies and fold axial surfaces as in Fig. 2.

(a) Early stage of D_1 : the Ela nappe is thrust over the Err-Carungas nappe from east to west, perpendicular to the plane of the section. An internal thrust forms in the Ela nappe, bringing the Üertsch element (ÜE) over the Compass element (CE). D_1 folds forming during this stage face towards south. The "Subsilvretide Linsen" (SSL) are interpreted as representing the extremely thinned inverse limb of a south-facing syncline comprising the entire Üertsch element.

(b) Late stage of D_1 : structures in the Ela nappe are steepened by upright folds, the Tschitta anticline (TA) and a syncline south of it. The area was later overprinted by recumbent D_2 folds, leading to the geometry seen in Fig. 3b.

thrust within the Ela nappe that brought the Üertsch element over the Compass element is also ascribed to this stage (Fig. 8a). We relate the south-facing D_1 folds and the internal thrust to formation and transport of the Ela nappe, and assume that the direction of shearing was towards west. This is indicated by the general east-west orientation of the D_1 stretching lineation not only in the Ela nappe but also in the over- and underlying units. Note that the termination of the Compass element towards north (Fig. 8a) has to be interpreted in terms of a lateral ramp in this case.

How can the southward facing direction of D_1 folds be reconciled with westward thrusting? We assume that the parallelism of the fold axes and stretching lineations is the result of a systematic rotation of the former towards the shearing direction. If folds had been initiated with axes perpendicular or oblique to the shearing direction, and with a facing towards west, the present southward facing requires that the fold axes were rotated uniformly and counterclockwise in map view.

The folds described above have axial planes subparallel to the thrust surface along which the Ela nappe was emplaced on the Err-Carungas nappe, and also to the internal thrust of the Üertsch element over the Compass element. A different class of D_1 folds must have developed after the Ela nappe had been emplaced on the Err-Carungas nappe. These younger folds deform the basal thrust of the Ela nappe (Fig. 3b, Fig. 8b). The folds are also attributed to D_1 , because a distinction between the two sub-generations is only possible in a few places, and because they probably formed in a continuous process. One of the younger D_1 folds is the east-plunging Tschitta anticline. It forms a half-window in which Upper Jurassic to Cretaceous sediments of the Err-Carungas nappe appear under the Ela nappe (Fig. 2, coord. 779/163, and Fig. 3b). The younger folds are

responsible for the general steepening of rock units not only in the Ela nappe, but also in the northernmost parts of the Err-Carungas nappe. In the following, this belt of steep units will be termed “Albula steep zone”.

The development of D_1 structures in the Ela nappe can be summarized as follows: the Ela nappe was detached from its basement along the Carnian evaporite, and transported towards west. Early D_1 folds and an internal thrust of the Üertsch element over the Compass element evolved during this detachment and transport of the nappe. Later on, after emplacement of the Ela nappe on the Err-Carungas nappe, upright folds developed, leading to a general steepening of rock units (Albula steep zone).

3.2.3 D_2 “collapse folding” and minor normal faulting in the Ela nappe

D_2 folds of the Ela nappe are typically open to tight, rarely isoclinal with subhorizontal to moderately dipping axial surfaces (Figs. 9a, 10b). In pelitic lithologies, they are associated with a solution- or crenulation cleavage. Open D_2 folds often have no axial-plane cleavage. Many of the D_2 fold axes are oriented east-west, parallel to D_1 folds and the D_1 stretching lineation (Figs. 7b, 10a). However, the trend of D_2 folds is highly variable, and almost north-south striking axes occur as well. Figure 9a shows D_2 folds trending obliquely to D_1 structures and therefore deforming the D_1 lineation. The facing directions of east-west trending D_2 folds vary depending on their position in respect to upright D_1 folds like the Tschitta anticline. D_2 folds face north on the northern limbs of upright D_1 anticlines, and south on the southern limbs (Fig. 3b). The facing direction of more north-south oriented D_2 folds is generally towards east (Fig. 7b).

The most spectacular and obvious D_2 structure is the east-west-striking, north-facing, recumbent Ela fold marked by the thick Hauptdolomit of Piz Ela. Previously this fold was interpreted to be related to the formation of the Ela nappe as a recumbent fold nappe (“Stirnfalte” or frontal fold of the older authors, e. g. Heim 1922, Fig. 227; Eugster 1923, Fig. 32). However, the fold clearly overprints D_1 folds, and the D_1 cleavage is folded around its hinge. It must therefore be younger than D_1 , as was already proposed by Spitz & Dyhrenfurth in their very remarkable article on the tectonics of the Ela – Silvretta area (1913, p. 498).

Large-scale D_2 folds deform the base of the Silvretta nappe west of Bergün, representing the preserved original thrust of the Silvretta over the Ela nappe formed during top-west to top-northwest displacement. For example Figure 3a shows the Silvretta basal thrust folded around the Ela D_2 fold (see also cross section of Piz Ela in Trümpy 1980, p. 238). However, further east where the Silvretta base was reactivated by top-east displacement and where it coincides with the continuation of the Ducan normal fault, axial surfaces and cleavage of D_2 folds become subparallel to the Silvretta base. Folding of the Silvretta base by D_2 is no more observed. This is one piece of evidence amongst others indicating that D_2 folding in the Ela nappe postdates the emplacement of the Silvretta on the Ela nappe, but is contemporaneous with the extensional faulting in the Silvretta nappe.

A crucial outcrop for understanding the relation between D_2 folds and extensional faults at a smaller scale is Igl Compass north of Albula pass (Fig. 11). Here, the D_2 fold axes strike north-northwest. The Jurassic strata of Igl Compass form a large, northeast-facing D_2 anticline with a moderately northeast-dipping axial surface. Along the fault

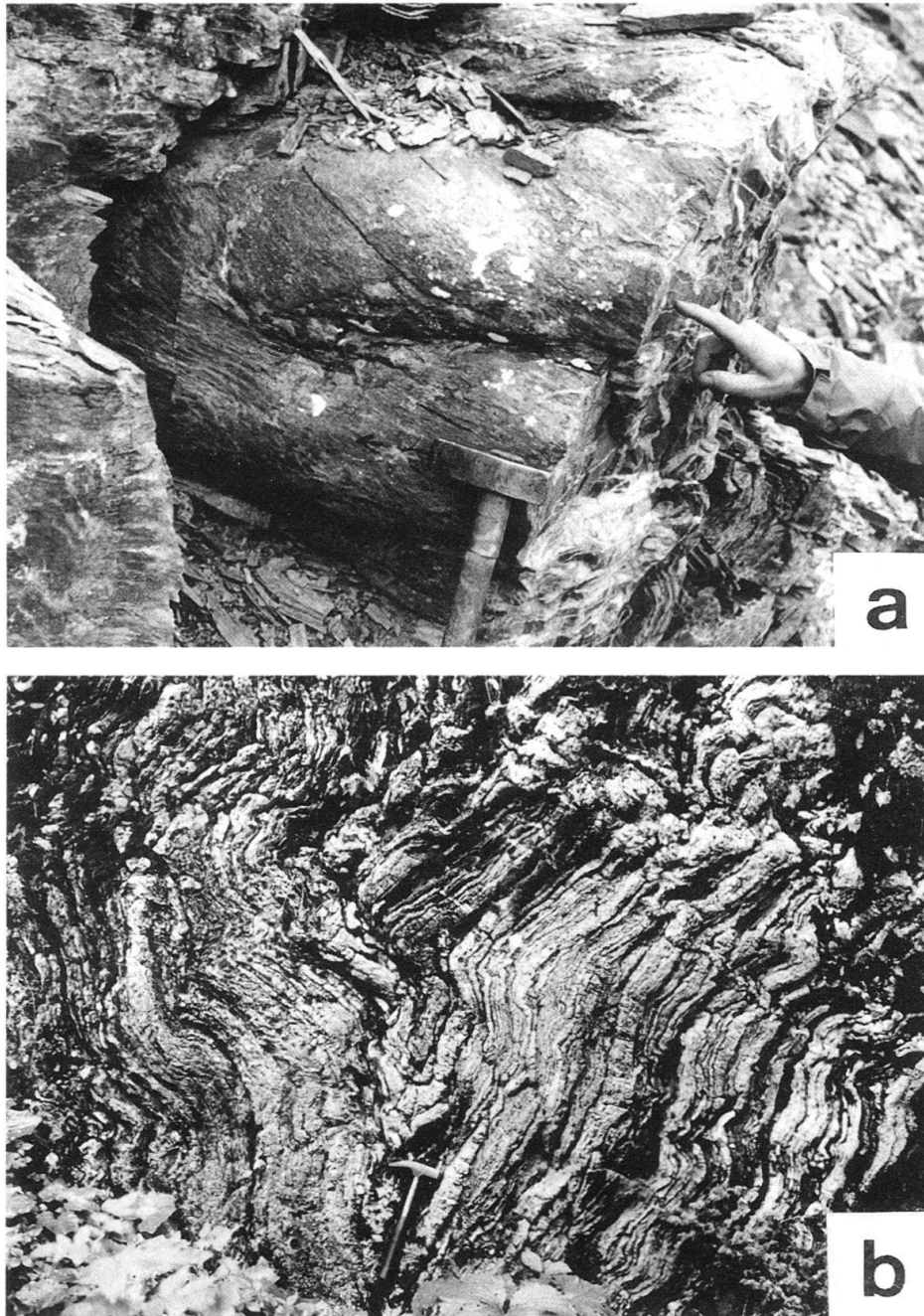


Fig. 9. (a) D_1 – D_2 overprinting in the Ela nappe. Recumbent D_2 folds in limestone of the Allgäu Formation on the south side of Igl Compass (coord. 782.9/162.5). The marked lineation curving around the fold hinges is the D_1 stretching- and cleavage/bedding intersection lineation.

(b) D_1 – D_2 overprinting in the Err-Carungas nappe. Upright D_1 synform in Upper Jurassic radiolarite of the Carungas zone, overprinted by weak D_2 folds with subhorizontal axial surfaces. The D_1 fold is a minor fold in the northern limb of the Tschitta anticline (compare Fig. 3b). Outcrop under the third railroad bridge over the road from Bergün to Albula pass near Punt Ota (coord. 777.6/163.3).

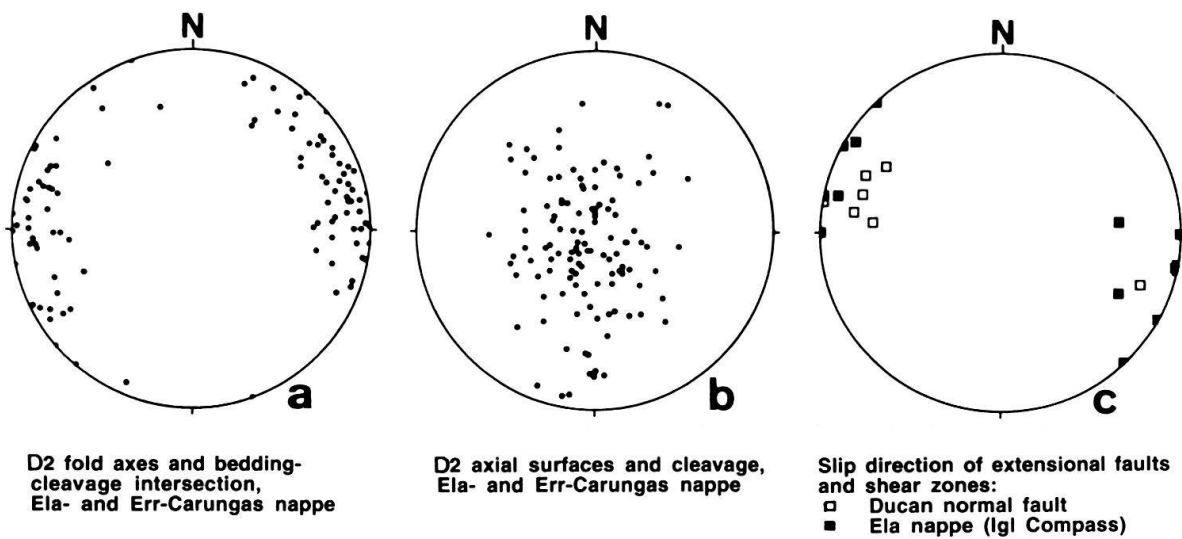


Fig. 10. Equal-area, lower-hemisphere stereographic representation of D₂ structures in Ela nappe and Err-Carungas nappe. Note parallelism in (c) between slip direction of Ducan normal fault (open symbols) and D₂-related shear zones and normal faults in the Ela nappe (filled symbols). For further explanation see text. After Froitzheim (1992).

contact shown in the upper right corner of Figure 11, the Jurassic strata are overlain by Triassic dolomite. This contact is a top-to-the-east-southeast directed normal fault, as indicated by asymmetric shear-band/foliation relations and drag folds in mylonitic limestone along the fault. The normal fault overprints a former thrust, the thrust of the Üertsch element over the Compass element (see above). As a result, it has older rocks in the hanging wall than in the footwall. It is subparallel to the Ducan normal fault further north and has the same slip direction (Fig. 10c). Therefore it is interpreted as a normal fault of the same generation as the Ducan fault. Tentatively, a second fault in a deeper structural level is also interpreted as a normal fault (Fig. 11). Parasitic D₂ folds subordinate to the northeast-facing anticline are seen between the two faults. These minor folds are associated with extensional shear zones generally located in the overturned limbs of the folds and resulting in stretching and thinning, or complete disruption, of the overturned limbs. The regular arrangement of the shear zones in the overturned limbs of the folds makes it likely that both kinds of structures developed together.

The development of the Igl Compass structure is explained in Figure 11b. Because Igl Compass is located near the hinge of a large-scale, upright D₁ fold with an east-dipping axis (the Tschitta anticline), it is assumed that the strata dipped east or northeast before D₂. Deformation in a broad shear zone with a normal-fault geometry, dipping toward east at a shallower angle than the bedding, resulted first in shortening and buckling of the competent layers. Later, with progressive deformation, the layers rotated into the extension field of the incremental strain ellipse and were disrupted by extensional shear zones. In summary, the geometric relations between shear zones and folds at Igl Compass suggest that fold formation resulted from top-to-the-east-southeast directed extensional shearing, affecting initially east- to northeast-dipping layers (Froitzheim 1992).

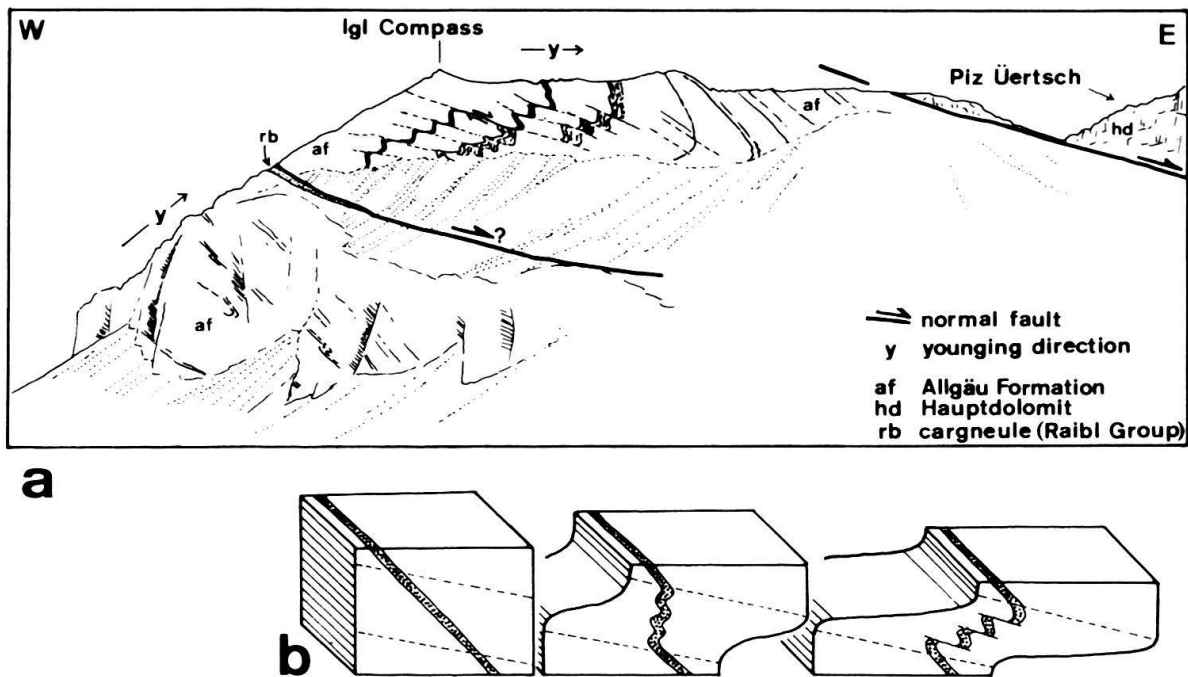


Fig. 11. D₂ structures at Igl Compass (Ela nappe north of Albula pass). (a) View of Igl Compass from south. Note regular arrangement of extensional shear zones in hinges of folds, suggesting that folds and shear zones originated from continuous process. (b) Model for continuous development of D₂ folds and extensional shear zones by top-east directed shearing deformation. Stippled layer is first shortened, then extended. After Froitzheim (1992).

This explanation can be extended to the D₂ folds of the Ela nappe in general (Froitzheim 1992): These folds reflect east-southeast directed extension whereby previously steepened layers (Albula steep zone formed during D₁) were shortened in a subvertical direction.

3.2.4 D₃ folding in the Ela nappe

D₃ folds are open folds with steeply dipping axial surfaces, affecting the Silvretta, Ela and Err-Carungas nappes together. D₃ fold axes and axial surfaces in the Ela nappe strike east to southeast. A cleavage related to D₃ was not observed. The style of D₃ folding is strongly dependent on the lithology of the rocks affected. The thick Hauptdolomit of the Ela nappe west of Bergün is unaffected by D₃ folding while the Allgäu Formation of Piz Blaisun (Fig. 2, coord. 785.7/164.2) is particularly intensely folded by D₃ (Pittet 1993, Unmüssig 1993). The syncline at the summit of Piz Blaisun, with Upper Jurassic radiolarite in the core, is such a D₃ structure. This syncline has a vertical axial surface; others have steeply north- or south-dipping axial surfaces.

The structural analysis of the Ela nappe thus reveals the superposition of three major deformation events. The first is related to westward thrusting and subsequent steepening of the rock units in the "Albula steep zone", the second one to east-southeast directed extension, and the third one to renewed shortening in a north-south to northeast-southwest direction.

3.3 *Err-Carungas nappe*

3.3.1 General description

The Err-Carungas nappe includes the “Errdecke s.s.”, the “Albulalappen” and the underlying “Carungasdecke” as defined by Stöcklin (1949, Tf. 1, “Tektonische Übersicht”). We treat these units as parts of one nappe, because in Val d’Err (Fig. 2), Carungas zone and Err nappe s. s. are connected by a continuous syncline of Jurassic-Cretaceous sedimentary rocks (Lozza 1990). Important displacement horizons may exist, however, in the lower part of the Carungas zone (G. Eberli, pers. comm.; see also Ring et al. 1990). The basement of the Err nappe s. s. and the “Albulalappen” are formed by Late- to Post-Hercynian granitoids and their wall rocks of gneiss and mica schist. A thin cover of Triassic rocks is preserved on top of this basement and along its northern border near the Albula pass. The Carungas zone is exposed in an eastward-narrowing stripe between the Err nappe s. s. and the “Albulalappen” to the south and the Ela nappe to the north (most of the area labelled “Mesozoic sedimentary rocks” in Fig. 2). This zone is made up of intensely folded, exceptionally thick Upper Jurassic to Cretaceous sedimentary rocks with thin anticlinal cores of Lower to Middle Jurassic, Triassic and basement rocks. In the Middle Jurassic, the area of the present Err-Carungas nappe was the site of dramatic rifting activity. This is documented by erosional hiatuses (Stöcklin 1949), sedimentary breccias with basement clasts, and preserved normal faults. Remnants of a low-angle detachment fault of presumably Middle Jurassic age are found on top of the Err nappe s. s. around Piz d’Err and Piz Jenatsch (Froitzheim & Eberli 1990).

3.3.2 Structural analysis

Because of the complicated rift configuration, the early Alpine (pre- D_2) deformation of the Err-Carungas nappe is only poorly understood. In pelites and pelitic limestones (e. g. *Aptychus* limestone) of the Carungas zone, a well developed early cleavage has often completely transposed sedimentary bedding. D_1 folds associated with this cleavage are isoclinal and some of them have the geometry of sheath folds. The orientation of D_1 folds is highly variable, due to their sheath-fold geometry and the strong D_2 overprint. The most prominent D_1 structure of the Carungas zone is the Tschitta anticline. In the east (Fig. 3b) the Tschitta anticline deforms the thrust at the base of the Ela nappe and has an upright, east-west striking axial surface. Further towards the southwest, the axial surface becomes sub-horizontal (Fig. 3a). The continuation of the Tschitta anticline in Figure 3a is hypothetical. In contrast to the sedimentary rocks of the Carungas zone, the pre-Permian basement mass of the Err nappe s. s. is devoid of penetrative D_1 structures (G. Manatschal, pers. comm.).

D_2 structures of the Err-Carungas nappe are similar to those of the Ela nappe: recumbent folds with an axial plane solution cleavage or crenulation cleavage. Typically, recumbent D_2 folds overprint upright D_1 folds in a type 3 pattern (Ramsay 1967; Fig. 9b). The frontal fold of Piz d’Err (Fig. 3a, right-hand end of section) is such a major, north-facing D_2 anticline. D_2 folding also affected the boundary between Err-Carungas nappe and Platta nappe: a half-window exposing the Platta nappe in Val d’Err (Fig. 2, coord. 773/160) represents the eroded core of a D_2 fold (Fig. 3a). These folds are interpreted as reflecting vertical shortening of previously steepened layers during east- to southeast-directed extension, just like the D_2 folds of the Ela nappe.

D₂ normal faults similar to those observed in the Silvretta nappe and also, but to a much lesser extent, in the Ela nappe, have recently been found in the Err-Carungas nappe (Weh 1992, G. Manatschal, pers. comm.). Weh (1992) reported a subhorizontal, top-southeast directed cataclastic shear zone near Murtelet Triged (Fig. 2, coord. 779/161) in the northern part of the Err basement and ascribed it to extensional faulting coeval with D₂ folding. It is possible that more such extensional faults and shear zones, related to D₂ deformation, exist in the northern Err-Carungas nappe.

D₂ and D₁ structures are overprinted by upright, open folds with east- to southeast striking and steeply north- to northeast-dipping axial planes (D₃). D₃ folds in the Err-Carungas nappe are associated with a weak axial plane solution cleavage. The broad anti-formal arch described by the D₂ axial surfaces in Figure 3a is a D₃ structure.

The Err-Carungas nappe thus shows a structural evolution very similar to that of the Ela nappe: early thrusting and folding (D₁) were followed by recumbent “collapse folding” (D₂) and by still later, open D₃ folding.

4 Sequence of stages of the orogenic evolution

In the preceding paragraphs, we have described the sequence of deformation phases observed in each of the three nappes, Silvretta, Ela and Err-Carungas. We will now combine these data and propose a reconstruction of the regional tectonic evolution, assuming that the deformation phases are related to distinct stages of the orogenic evolution.

4.1 *Trupchun phase (D₁): Cretaceous top-west thrusting and folding*

The Trupchun phase includes the D₁ thrusts and folds of the three nappes. It is named after Val Trupchun, situated at the western end of the Ortler nappe (see chapter 5.3), where structures of this phase are particularly well preserved.

We assume that the D₁ folds of the Silvretta nappe, such as the Ducan syncline, were formed during initial detachment and westward transport of the nappe. Their orientation – northeastern strike and northwestward facing – fits well together with the westward to northwestward direction of thrusting, as indicated by the lineation in the older, higher-temperature mylonites at the base of the Silvretta nappe. D₁ folds in the Ela nappe are more complicated. In the Ela nappe, D₁ includes two kinds of folds: first, east-striking, south-facing folds with axial planes subparallel to the basal thrust of the Ela nappe, and second, also east-striking, but upright folds deforming the basal thrust (Fig. 8).

The first “sub-generation” is comparable and probably coeval with the D₁ folds of the Silvretta nappe. The different strike of the fold axes, northeast in the relatively rigid Silvretta nappe and east in the ductile Ela nappe, can be explained with a rotation of fold axes of the Ela nappe into the shear direction. The beginning of such a rotation is noticed in the southwestern part of the Ducan syncline, where fold axes curve around from northeast-striking to north- and northwest-striking. A possible explanation for the anti-clockwise rotation of fold axes is a different rate of top-west shearing, higher in the north and lower in the south. This implies that northern parts of the nappe pile advanced towards west relative to more southern parts.

The slightly younger, upright D₁ folds in the Ela nappe have no counterpart in the Silvretta nappe. These upright folds led to a steepening of all rock units in the Albula

steep zone, comprising the presently exposed Ela nappe and the northernmost part of the Err-Carungas nappe. D_1 in the Err-Carungas nappe is very similar to D_1 in the Ela nappe, except for a strong decoupling between the basement, remaining undeformed, and the sediments of the Carungas zone, where the occurrence of sheath folds indicates relatively higher strains.

Strictly, it would be possible to split the Trupchun phase in two phases, one for the initial thrusting and one for the formation of the Albula steep zone. Such a distinction, however, is feasible only in a few places. Therefore we prefer to interpret the initial thrusting and the formation of the Albula steep zone as a continuous process that only locally led to geometric overprinting relations.

The age of the Trupchun phase is Late Cretaceous. The youngest biostratigraphically dated sediments in the Carungas zone are Lower Cretaceous (Stöcklin 1949). Good constraints on the age of this phase exist in the Engadine Dolomites (see chapter 5).

4.2 Ducan-Ela phase (D_2): Late Cretaceous east-west extension

Since Eugster (1923) recognized the normal faults of the Silvretta nappe, several authors have tried to explain these faults in the context of crustal shortening (Eugster 1923, Heim 1922, Eichenberger 1986). Eugster (1923) created the new term “Untervorschiebung” (“underfore-thrust”) for these faults, implying that they are basically related to thrusting. The drawing by Heim (1922, Fig. 229) suggests a systematic relation between folds – the D_1 folds of the Ducan area – and normal faults, in the way that the normal faults are parallel to the axial planes of the folds. Such a systematic relation, however, does not exist: the Ducan normal fault cuts obliquely through the Ducan syncline.

The D_2 normal faults of the Silvretta postdate Trupchun-phase crustal shortening and are related to subsequent east-southeast directed crustal extension, for the following reasons: (1) The faults clearly overprint the dominant D_1 folds and the basal thrust of the Silvretta, so that their formation cannot be related to folding and thrusting as envisaged by Heim (1922) and Eichenberger (1986). (2) The normal faults are not restricted to deformation within the Silvretta nappe. The Ducan normal fault additionally reactivated the Silvretta basal thrust, a process that transported the Silvretta nappe back towards east-southeast relative to deeper units.

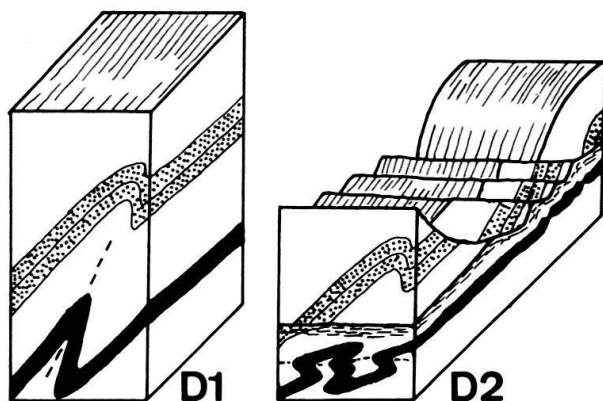


Fig. 12. Model for contemporaneous development of normal faults and second-generation folds during crustal extension. Left: earlier, upright folds of the Trupchun phase; right: extension and thinning of the crust in the Ducan-Ela phase, leading to normal faulting in an upper layer and to formation of recumbent second-generation folds below. The contact between the two layers is a low-angle extensional shear zone (cf. Silvretta base east of Bergün).

D₂ structures in the Ela and Err-Carungas nappe are recumbent folds and, to a minor extent, top-east-southeast directed low-angle normal faults. It was shown above that the recumbent folds developed together with the normal faults, and reflect horizontal extension and vertical shortening of steeply inclined layers. We assume that D₂ folding of the Ela and Err-Carungas nappes and normal faulting within the Silvretta nappe resulted from the same event of crustal extension. The different style of deformation can be explained in the following way: normal faulting in the Silvretta unit reflects brittle extension in a higher crustal level, whereas D₂ folding within the Ela and Err-Carungas nappes documents ductile extension in a deeper crustal level. The low-angle part of the Ducan normal fault acted as a décollement horizon separating the two levels (Fig. 12). Apart from the depth of burial, the style of extension also depends on the lithological composition of the nappes (Weh 1992): The Ela and Err-Carungas nappes, comprising sedimentary rocks with extreme competence contrasts (dolomite versus shale) and lacking a pre-Mesozoic basement, are more likely to develop folds than the basement-dominated Silvretta nappe. In addition, rock units had been steepened during D₁ in the Ela and Err-Carungas nappes, but not in the Silvretta nappe. Such steepening is a pre-requisite for “collapse folding” (Froitzheim 1992).

The ductile thinning in the Ela and Err-Carungas nappes was not coaxial, but had a component of top-east-southeast directed shearing, as indicated by the generally eastward transport direction of the minor normal faults associated with the D₂ folds. This offers an explanation for the eastward facing direction of north-south striking D₂ folds in the Ela nappe (Fig. 7b).

The extensional event responsible for normal faulting in the Silvretta and D₂ folding in the Ela and Err-Carungas nappes, the Ducan-Ela phase, is probably Late Cretaceous in age. Evidence for this age will be provided below (chapter 6.1.3). At this stage it is important to note that the Ducan-Ela phase predates renewed north-south shortening during the Blaisun phase.

4.3 Blaisun phase (D₃): Early Tertiary north-south shortening

This phase produced the east- to southeast-striking D₃ folds observed in all three nappes. This folding is particularly intense and beautifully exposed at Piz Blaisun and is therefore referred to as “Blaisun phase”. Within the Ela nappe the intensity of Blaisun-phase folding decreases towards west (compare Figs. 3a and b). Blaisun-phase folding resulted in the present synformal shape of the Ducan normal fault. The age of the Blaisun phase is Early Tertiary (see below, chapter 6.2).

4.4 Turba phase (D₄): Renewed east-west extension

Above we have discussed the three most important stages of deformation in the area of the Silvretta, Ela and Err-Carungas nappes. The following phases have only weakly modified the internal geometry of the Austroalpine, but have strongly affected the Austroalpine-Penninic boundary zone.

A second phase of top-east-directed extensional faulting is documented by the Turba mylonite zone, an east-dipping normal fault between the Platta nappe above and the Arblatsch flysch below (Fig. 1, Nievergelt et al. 1991 and in press, Liniger 1992). The Turba

mylonite, best exposed at Piz Turba between the Oberhalbstein and Bergell valleys (outside the map, Fig. 2), is a calc-mylonite with quartz clasts. Stretching lineation and shear-sense criteria indicate down-to-the-east displacement of the hanging wall comprising Platta nappe and Austroalpine, relative to the Middle Penninic units in the footwall (Liniger 1992). The northern continuation of the Turba mylonite zone is indicated between the Platta nappe and underlying Arblatsch flysch in the southwestern part of the map, Figure 2, and in Figure 3a. Vitrinite reflectance of samples from this area indicates an abrupt decrease of Alpine metamorphic temperatures from the footwall to the hanging wall across the Turba mylonite zone (measurements by R. Ferreiro Mählmann, in Nievergelt et al. in press), compatible with normal fault movement. Still further towards north, the continuation of the Turba mylonite zone is unclear. The extreme thinning of the nappe units east of Tiefencastel (Trümpy 1980, p. 237), where the Ela nappe is represented by only a few metres of Jurassic limestone, overlain by Triassic dolomite of the Silvretta nappe and underlain by a serpentinite-bearing shear zone, strongly suggests that the Turba mylonite zone continues towards the north along the base of the Austroalpine. Late-stage, top-east shearing probably related to the Turba phase was also observed in the Arosa zone near Arosa and along the western border of the Err nappe (Ring et al. 1991, Dürr 1992). The Turba normal fault truncates Blaisun-phase folds in the Margna and Platta nappe near Septimer pass (Liniger & Nievergelt 1990, p. 97; D_2 of these authors corresponds to the Blaisun phase).

Normal faults of the Turba phase have orientations similar to the ones of the Ducan-Ela phase and are therefore easily confounded with these. The two generations of normal faults can only be distinguished by using overprinting relations with folds of the Blaisun phase: Ducan-Ela-phase normal faults are deformed by Blaisun-phase folds (see Fig. 5), whereas the Turba normal fault truncates such folds.

4.5 Domleschg phase (D_5): Late-stage northwest-southeast shortening

The Domleschg phase, originally defined by Pfiffner (1977) in the North Penninic Bündnerschiefer of Graubünden, corresponds to the latest compressional overprint recognized in the Middle Penninic Schams nappes (D_3 of Schmid et al. 1990). Northeast-striking, open folds with constant northwestward vergence and southeast-dipping axial planes only achieve moderate shortening. These folds can be continuously traced from the Schams area towards the east and into the Austroalpine units in the Tiefencastel area. A major Domleschg-phase syncline extends from Piz Toissa northeast into the Silvretta nappe (Fig. 2, coord. 765/168; "Suraver Deckenmulde" of Ott 1925). The preservation of the Toissa klippe, a remnant of the Ela nappe on top of Penninic units west of the Julia valley (Fig. 2), results from its position within this syncline.

The Domleschg phase postdates the Turba phase. South of Piz Turba, the Turba mylonite zone is folded around an east-west striking antiform correlated with the Schams D_3 , and thus the Domleschg phase, by Liniger (1992, "M" in Fig. 15d).

5 Comparison with the Engadine Dolomites

In the following, we will compare the structures observed in the Silvretta, Ela, and Err-Carungas nappes with the ones of the Engadine Dolomites. Thereby we will attempt a

correlation of deformation phases across the Engadine line (Trümpy 1977, Schmid & Froitzheim 1993), a major discontinuity in the Austroalpine nappe pile of Graubünden. Furthermore, the Engadine Dolomites yield additional information about the geometry and timing of Trupchun-phase thrusting, because of the relatively minor post-nappe overprint as compared to the area described in the preceding chapters.

5.1 General description

The Engadine Dolomites (Fig. 13, Plate 1) represent a triangular-shaped area of Upper Austroalpine sedimentary rocks bounded to the northwest by the Engadine line, to the south and southeast by the basement of the Campo nappe, and to the northeast by the overlying Oetzal thrust mass, also formed by pre-Permian basement (Spitz & Dyhrenfurth 1914). Several thrust sheets are exposed in this area: from south to north, the Ortler, Quattervals and Sesvenna – S-charl nappe. The Zebbru thrust separates the lowermost thrust sheet, the Ortler nappe (predominantly Mesozoic rocks), from the underlying Languard and Campo basement nappes. The Trupchun-Braulio thrust defines the top of the Ortler zone and the base of higher thrust sheets, referred to as Quattervals nappe and Terza unit, sedimentary units of predominantly Late Triassic age. Towards east, the Quattervals nappe is interleaved with the Umbrail-Chavalatsch zone (Schmid 1973), a pile of often extremely thin thrust sheets or slivers in which the proportion of basement rocks derived from the Oetzal nappe increases from west to east. The largest basement sheet in this imbricate zone is the Braulio crystalline unit. North of the Quattervals nappe and the Umbrail-Chavalatsch zone follows the S-charl-Sesvenna nappe, divided from the former units by the Gallo line. Although the exact nature of the Gallo line is still dubious, it is well established that the Quattervals nappe and Umbrail-Chavalatsch zone are in a structurally higher position in respect to the S-charl-Sesvenna nappe (Schmid 1973). Hence, the Gallo line represents the basal thrust of the Quattervals and Umbrail-Chavalatsch units above the S-charl-Sesvenna nappe. Sesvenna and Campo basement thus occupy the lowermost structural position in the nappe pile of the Engadine Dolomites. An uncertainty exists about the importance of later extensional reactivation or overprint of the Gallo line, already assumed by Schmid (1973).

All subunits of the Engadine Dolomites can be traced into the footwall of the Schlinig thrust, forming the base of a higher Upper Austroalpine unit: The Oetzal nappe. The Zebbru thrust, the Trupchun-Braulio thrust, and the Gallo line merge into a mylonitic belt associated with the Schlinig thrust (“intra-basement shear zone”, Schmid & Haas 1989).

5.2 Correlation across the Engadine line

The geometric relations between Engadine Dolomites and the units northwest of the Engadine line have been subject to longstanding controversies (see discussion in Schmid & Haas 1989). A recent kinematic analysis of the Engadine line (Schmid & Froitzheim 1993) yielded movement vectors consistent with a sinistral strike-slip motion associated with a block rotation. This results in a component of downthrow of the Engadine Dolomites with respect to the Silvretta nappe. Retro-deformation of movements along the Engadine line yields the following nappe correlations: (1) The Ela nappe occupies a structur-

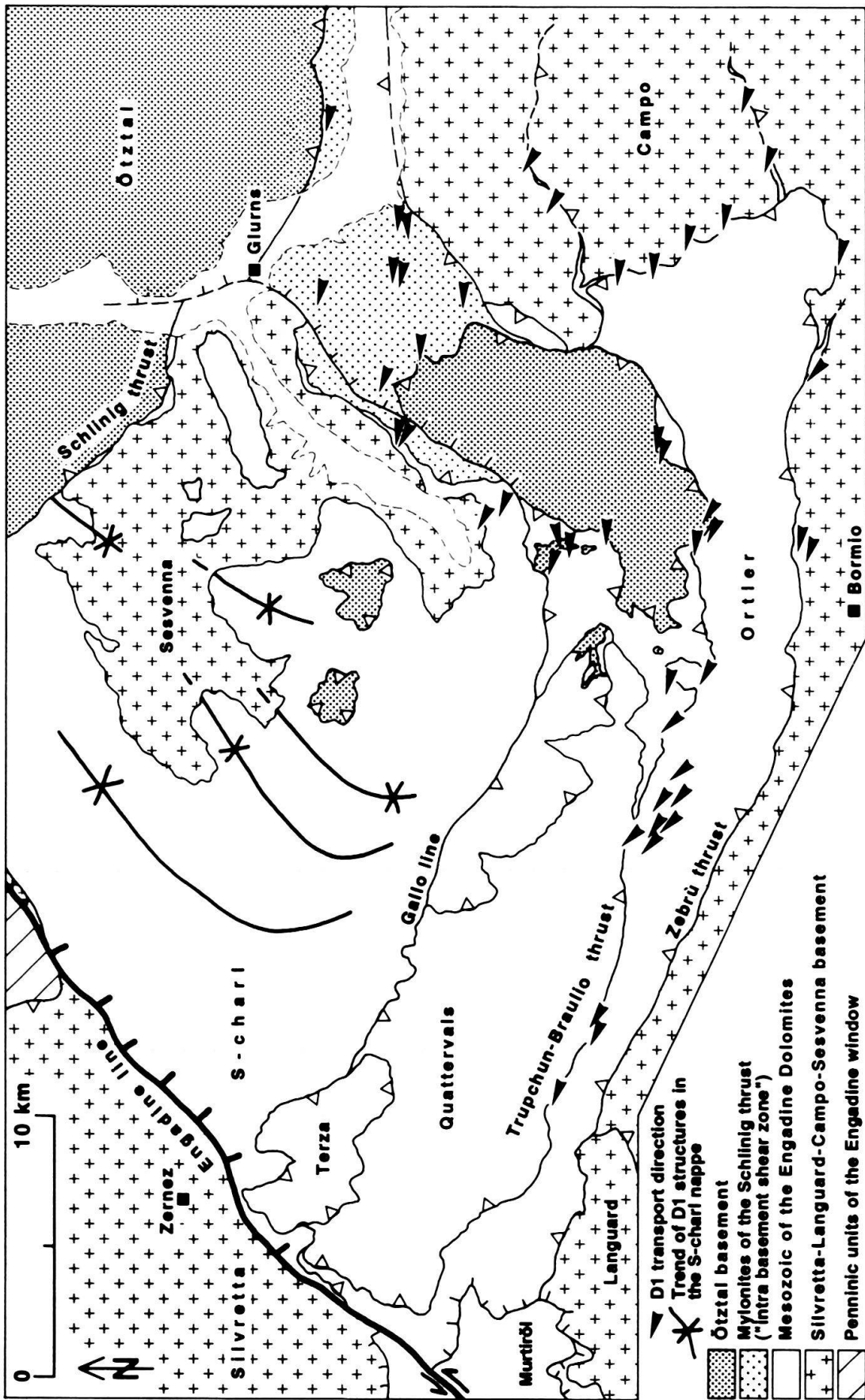


Fig. 13. Tectonic map of the Engadine Dolomites. Arrows indicate D1 transport directions as determined by microfabric analysis of mylonites and cataclases.

ally lower position in respect to the Engadine Dolomites and the basement thrust sheets of Languard and Campo, and has to be considered part of the Lower Austroalpine Bernina system (Fig. 1). This interpretation is contrary to the classical one, assigning the Ela nappe to the Upper Austroalpine (e. g. Spicher 1972: Tectonic map of Switzerland). Southeast of the Engadine line, the Triassic and Jurassic sedimentary rocks of the Corn unit represent a direct equivalent of the Ela nappe (Pl. 1). The Corn sediments are the uppermost element of the Bernina system, directly underlying the Languard basement. (2) The Sesvenna, Languard and Campo basement units are comparable to the Silvretta nappe regarding their tectonic position in the original nappe pile. (3) Equivalents of the Engadine Dolomites on the western side of the Engadine line were situated above the Silvretta basement and have been eroded away, with the exception of the Silvretta cover in the Ducan and Landwasser areas.

5.3 *Trupchun-phase folding and thrusting in the Engadine Dolomites*

Thrusting towards northwest to west and associated folding are particularly well exposed in the Ortler nappe. At the western end of this unit, in Val Trupchun, the local D_1 (Trupchun-phase) folds are open to isoclinal and associated with an axial plane cleavage. In contrast to the D_1 folds in the Silvretta cover, Trupchun-phase fold axes in the Ortler nappe have rotated towards parallelism with the transport direction by variable amounts. In stereographic representation the fold axes cover almost a complete great circle (Froitzheim 1988). Northwest-directed transport was deduced from an analysis of fold axis orientations (Froitzheim 1988). The different style of deformation during the Trupchun phase, when compared to the Silvretta nappe, is at least partly due to the different lithological composition: Lower to Middle Jurassic marls and limestones of the Allgäu Formation, predominant in Val Trupchun, contrast with the dolomite-dominated Triassic cover of the Silvretta nappe. A maximum age for the Trupchun phase in this area is given by the youngest sediments affected by these folds: Upper Cretaceous sediments occur in the core of a Trupchun-phase syncline in Val Trupchun. These are Cenomanian and possibly Middle Turonian foraminiferal marls (about 90 Ma, Caron et al. 1982), first described and termed "Couches Rouges" by Zoeppritz (1906). Therefore, thrusting and folding in the Ortler nappe began after 90 Ma.

The Trupchun-Braulio thrust at the top of the Ortler nappe and the Zebra thrust at the base of this nappe are both top-west to -northwest directed (Fig. 13), as is unambiguously demonstrated by kinematic analysis of calc-mylonites from the Trupchun-Braulio thrust and quartz mylonites from the Zebra thrust (P. Conti, work in prep.). Schmid (1973) and Froitzheim (1988) erroneously interpreted the Trupchun-Braulio thrust as a top-southwest backthrust, because Trupchun-phase folds are truncated by this thrust. At the eastern end of the Ortler nappe, Conti (1992) found a two-stage evolution of thrusting during the Trupchun phase: the Trupchun-Braulio thrust overprints earlier, also west-to northwest-directed thrusting along the Zebra thrust. Such a two-stage evolution of thrusting may account for the overprinting relation observed in Val Trupchun. Both the Trupchun-Braulio and the Zebra thrust can be continuously traced further towards east where the synkinematic metamorphic grade systematically increases and reaches the greenschist facies near the eastern margin of Figure 13 (Schmid & Haas 1989). They finally both merge with the eastern continuation of the Schlinig thrust, for which a Late

Cretaceous age of thrusting, between 100 and 80 Ma, is well constrained (e. g. Thöni 1986, review of radiometric ages in Schmid & Haas 1989).

Northeast-striking folds are dominant in the S-charl-Sesvenna nappe (Spitz & Dyhrenfurth 1914, Stutz & Walter 1983, Schmid & Haas 1989, see Fig. 13). These folds are the oldest Alpine structures in this area and can be attributed to the Trupchun phase. They are about perpendicular to the transport direction which was west-northwest to northwest as indicated by stretching lineations. The general style of the folds is very reminiscent of the Trupchun-phase folds in the Silvretta cover. In the area of the southern Sesvenna – S-charl nappe, a gradual change in the orientation of the Trupchun-phase folds is observed (Fig. 13): towards southwest, the folds curve from northeast-striking over north-striking to northwest-striking (Spitz & Dyhrenfurth 1914). This fold arc resembles the one observed at the southwestern termination of the Ducan syncline (Spitz & Dyhrenfurth 1913).

Locally within Permian to Lower Triassic pelites of the S-charl-Sesvenna nappe, a cleavage has developed under conditions of the lowermost greenschist facies. The formation of this cleavage is dated at 89 ± 5 Ma by K-Ar determinations on white micas (Thöni 1980), confirmed by ^{40}Ar - ^{39}Ar work (Thöni & Miller 1987).

5.4 Post-nappe deformation of the Engadine Dolomites

Unambiguous evidence for an extensional overprint during the Ducan-Ela phase has not been found yet within the Engadine Dolomites. Northwest-southeast-directed Alpine extension is observed in Upper Triassic dolomites of the S-charl unit (Schmid & Haas 1989) and the Ortler nappe (Froitzheim 1988). These authors attributed extension of the Upper Triassic dolomite layer to bookshelf- or domino-type antithetic faulting, related to Trupchun-phase thrusting. As discussed in Ratschbacher et al. (1989), local extension can be associated with non-plane-strain shearing, coupled with vertical thinning, in a large-scale overthrust shear zone. However, in the light of our recent discovery of crustal extension affecting a previously stacked pile of thrust sheets along the Ducan normal fault, such crustal extension during the Ducan-Ela phase cannot be ruled out as an explanation for some of the extensional structures in the Engadine Dolomites. We tentatively assume that both processes, thrust-related, local extension in the sense of Schmid & Haas (1989), and crustal-scale extension during the Ducan-Ela phase, left their traces in the Engadine Dolomites. Many of the southeast-dipping Alpine normal faults in the S-charl unit and in the Ortler nappe are restricted to the Hauptdolomit layer and do not continue in the over- and underlying strata. These faults probably formed during thrusting as proposed by Schmid & Haas (1989) and Froitzheim (1988). Some normal faults in the S-charl unit, however, cut down into the basement (see Fig. 5 in Schmid & Haas 1989) and may reflect crustal extension during the Ducan-Ela phase.

The local D_2 folds of the western Ortler nappe (Froitzheim 1988) are characterized by east- to southeast-trending axes and steeply south- to southwest-dipping axial planes. Very much analogous to the Blaisun-phase folds in the Ela nappe, these folds are responsible for tilting of previously flat-lying structural elements (in the Ela nappe, the axial planes of recumbent Ducan-Ela-phase folds) towards the north. Therefore this local D_2 can confidently be correlated with the Blaisun phase (D_3) defined in the Ela nappe. In the eastern part of the Ortler zone, Blaisun-phase folds are crosscut by dykes of mafic to

intermediate composition and calc-alkaline affinity (Conti et al. 1994). The dykes are about 32 Ma old (Dal Piaz et al. 1988). This age can hence be regarded as a minimum age of the Blaisun phase in this region.

Apart from the Engadine line, active near the Oligocene-Miocene boundary, and other brittle faults kinematically linked to this line (Schmid & Froitzheim 1993), no evidence for younger events is found in the Engadine Dolomites.

In summary, the structural architecture of the Engadine Dolomites is characterized by the strong prevalence of Trupchun-phase structures, including folds and west to north-west directed thrusts. The recumbent “collapse folds” of the Ducan-Ela phase are not observed in the Engadine Dolomites. On first sight, a striking similarity exists between the structural architecture of the Ela nappe and the one of the Ortler nappe: in both units, recumbent folds with north-dipping axial surfaces are the dominant structural elements. This similarity has misled several authors to regard the Ortler nappe as the continuation of the Ela nappe (e. g. Staub 1964, p. 87–88). The similarity, however, is only apparent: the recumbent folds of the Ortler nappe are thrust-related folds of the Trupchun-phase (D_1), whereas the recumbent folds of the Ela nappe are younger “collapse folds” of the Ducan-Ela phase (D_2). A correlation between northeast-striking folds in the S-charl-Sesvenna unit and the Ela “frontal fold”, as put forward by Heim (1922, Fig. 227), Eugster (1923, Fig. 32) and Staub (1924, Fig. 34) has to be rejected for the same reason: the first are Trupchun-phase folds, the latter belongs to the Ducan-Ela phase.

6 Synthesis: Structural evolution of the Austroalpine nappes in Graubünden

In the following, we extend our considerations to a larger area within the Austroalpine nappe pile in Graubünden. The sequence of deformation phases developed above applies also to other parts of this nappe pile. A correlation with the sequences established for the western border of the Err-Carungas nappe (Dürr 1992), the Samedan zone (Handy et al. 1993) and for the Margna nappe and surrounding area (Liniger 1992, Hermann & Müntener 1992) is given in Table 1. The correlation with the deformation sequence of the northern Malenco area east of the Bergell pluton (Hermann & Müntener 1992) is partly ambiguous because these authors observed one additional fold generation (D_4) that is not recorded in adjacent areas. It may represent a local phenomenon.

6.1 *Cretaceous orogeny*

6.1.1 From the Jurassic passive margin to the Late Cretaceous thrust belt

The domains of the Jurassic-age passive continental margin were telescoped by top-north-west to top-west directed thrusting in the Late Cretaceous Trupchun phase. This imbrication of nappes started after 90 Ma in the Ortler zone, as is indicated by the occurrence of Cenomanian to Lower Turonian “Couches rouges” in the core of a Trupchun-phase syncline in Val Trupchun (Caron et al. 1982; see above). The same is true for the Lower Austroalpine (Murtiröl half window and Samedan zone) where “Couches rouges” are overlain by flysch of probably Late Cretaceous age (Rösli 1927, 1946). The onset of flysch sedimentation indicates the beginning of convergence. These biostratigraphic data, together with radiometric ages from the Engadine Dolomites and the Schlinig thrust re-

Silvretta-Ela-Err (this article)	Western border of Err-Carungas nappe (Dürr 1992)	Samedan zone (Handy et al. 1993)	
Domleschg phase	--	F4 (folds)	
Turba phase	D3 (top-E normal faults)	steep, E-dipping normal faults	
Blaisun phase	D2 (folds)	F3 (folds), N-directed thrusts	
Ducan-Ela phase	--	F2 (folds), top-east extensional shear	
Trupchun phase	D1 (isoclinal folds, top-west shear)	F1 (folds), W- to SW-directed thrusts	
Silvretta-Ela-Err (this article)	Margna, Sella, Malenco (Hermann & Müntener 1992)	Margna, Platta, Avers NW of Engadine line (Liniger & Nievergelt 1990)	Schams nappes (Schmid et al. 1990, Schreurs 1993)
Domleschg phase		D3 (folds)	D3
Turba phase	D6 ("2nd phase of backfolding") D5 (top-east shear zones)	D2 (top-east Turba mylonite zone)	D2
Blaisun phase	D4 (folds) D3 ("First phase of backfolding")	F2 /D1 (folds)	D1
Ducan-Ela phase	D2 (top-east shear zones)	--	--
Trupchun phase	D1 (isoclinal folds)	F1 (isoclinal folds, top-W to top-SW mylonites)	--

Tab. 1. Correlation of deformation sequences.

ported above (chapter 5.3), indicate a westward migration of Trupchun-phase deformation: thrusting along the Schling thrust started at about 100 Ma, cleavage in the S-charl nappe was formed around 90 Ma, and the western Ortler nappe was buried under the higher thrust sheets after 90 Ma (Fig. 14).

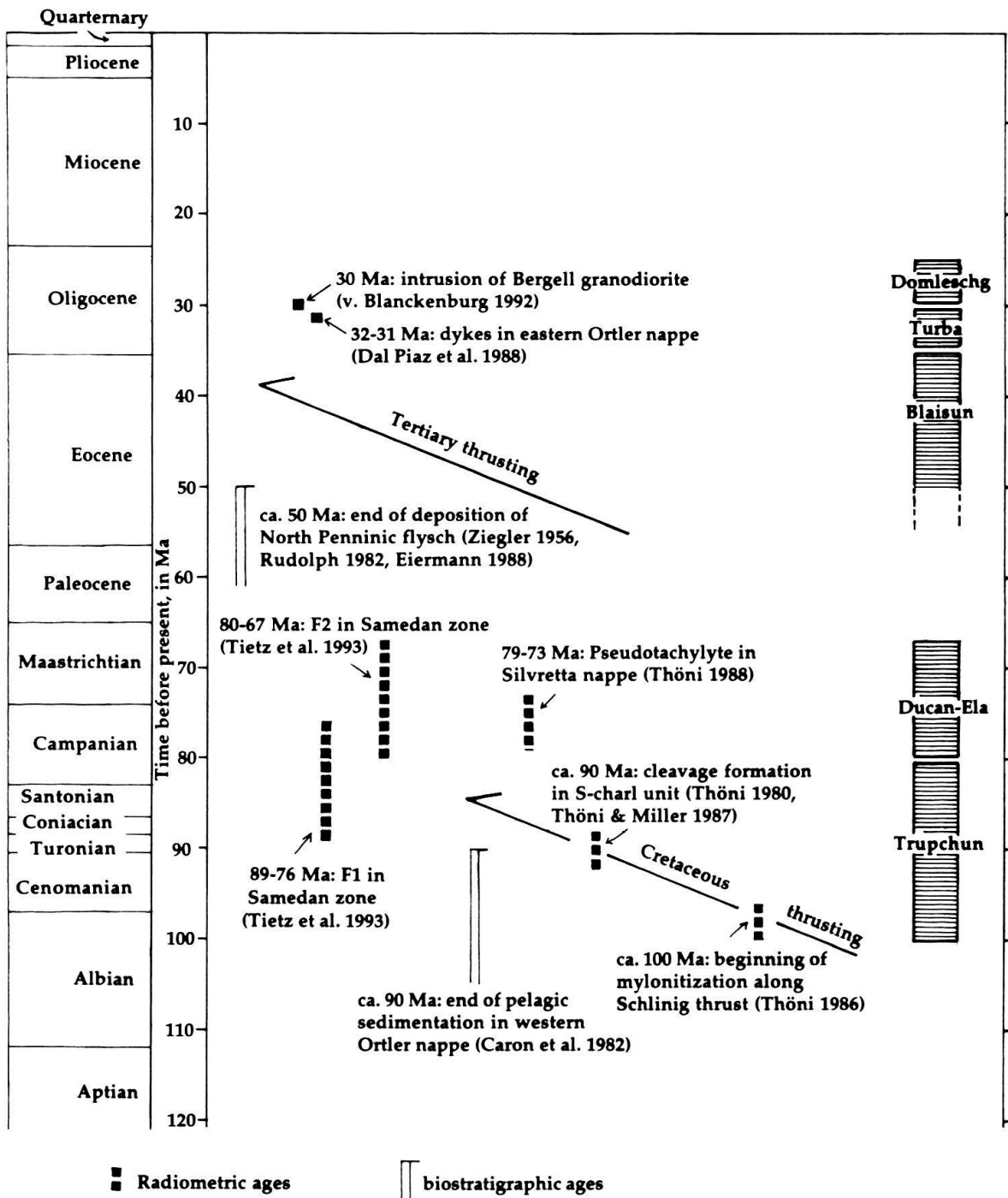
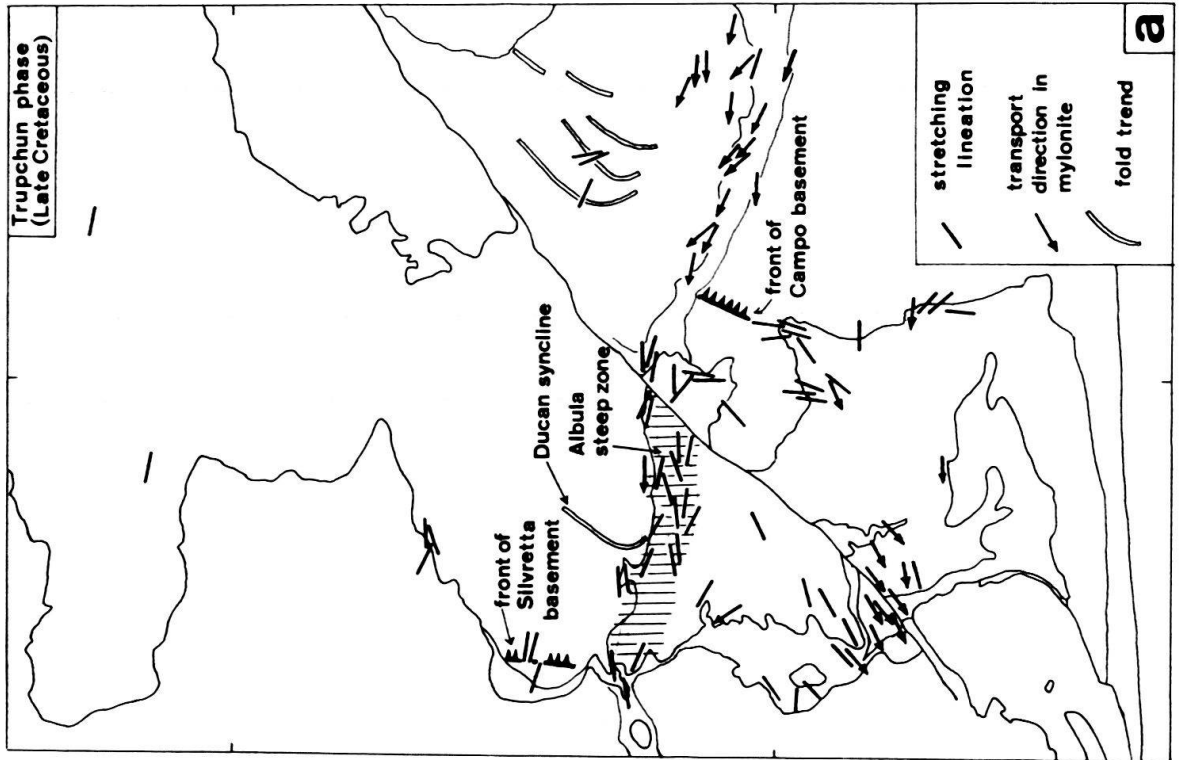
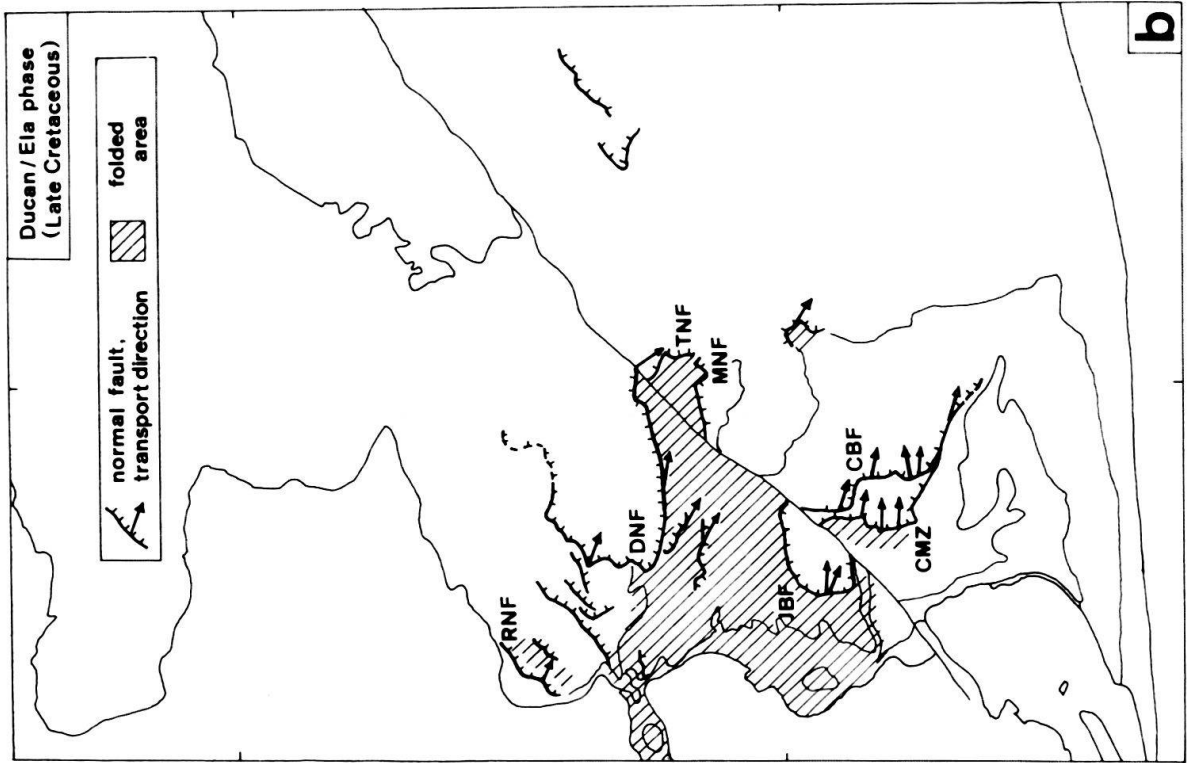
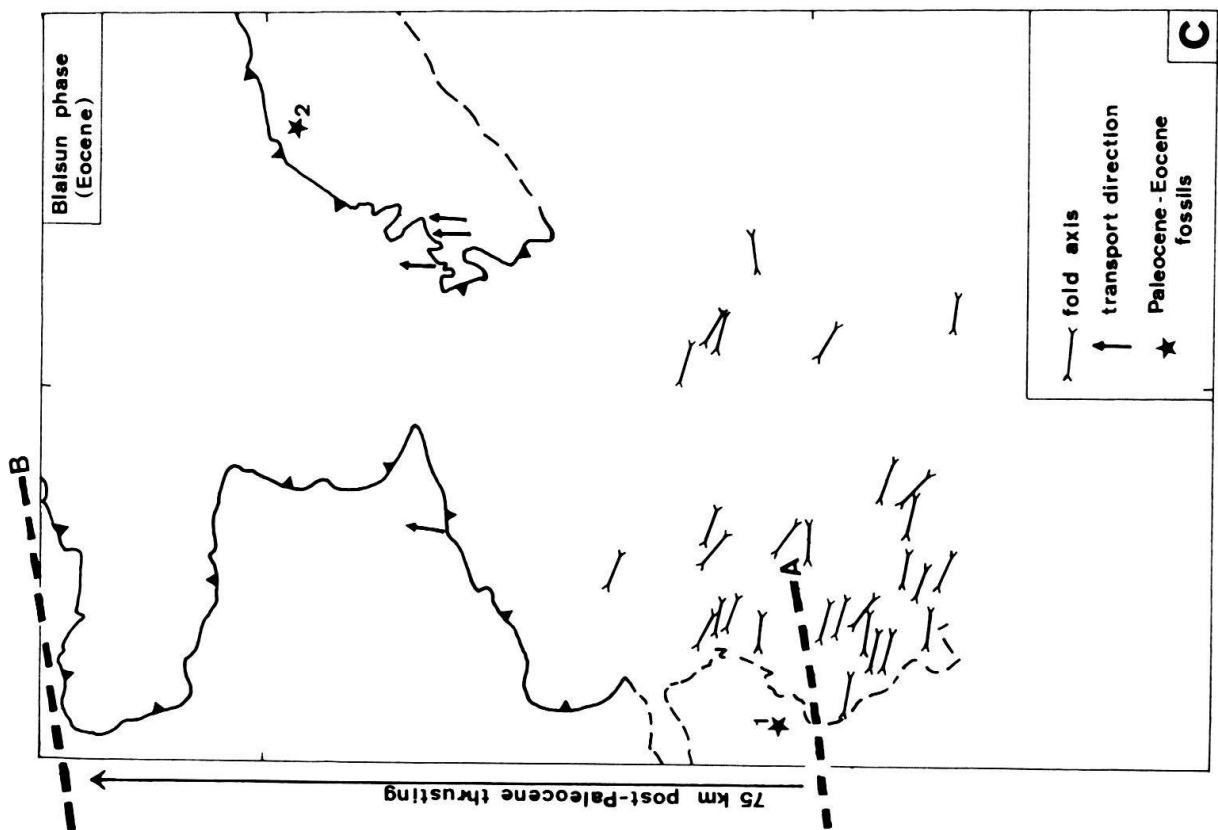
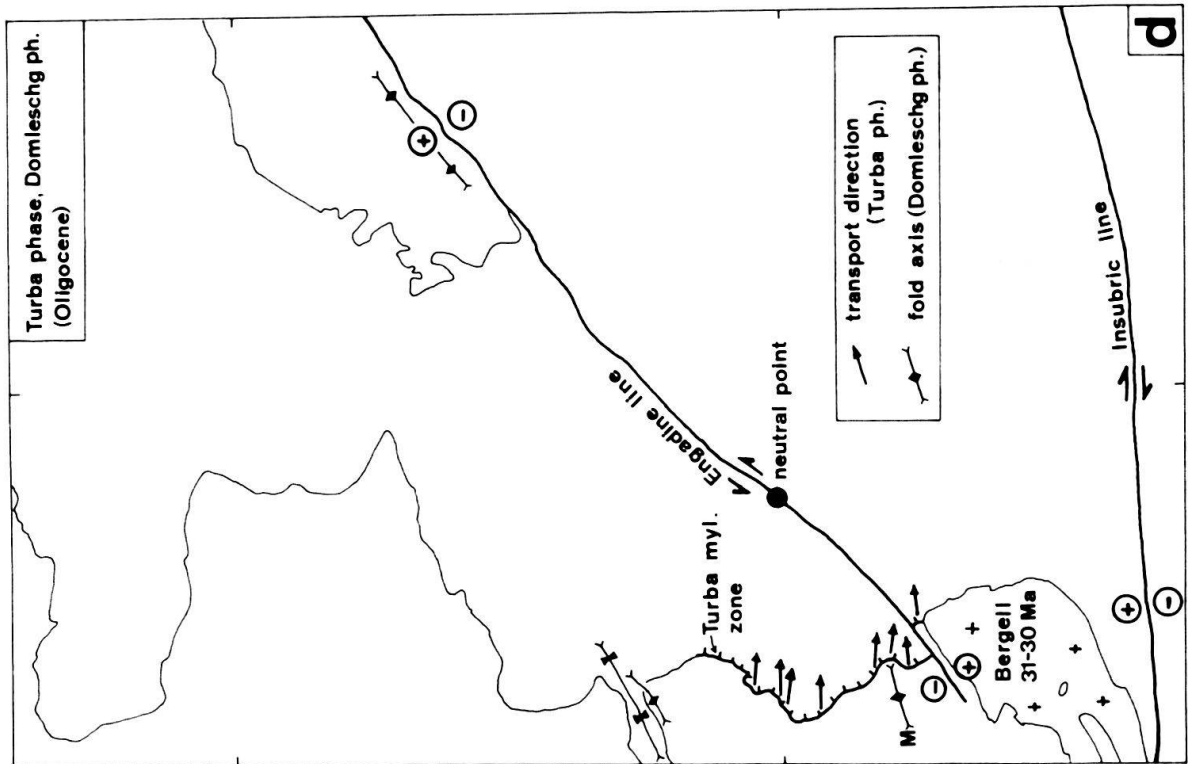


Fig. 14. Time table, showing radiometric and biostratigraphic age determinations and their relation to the deformation sequence of the Austroalpine units.

Most authors assume that oceanic lithosphere of the South Penninic ocean was subducted under the Austroalpine continental margin in the Cretaceous (Trümpy 1975, Frisch 1979, 1980). The subducted lithosphere carried the Margna-Sella continental fragment which collided with the Austroalpine mainland. The ophiolites of the Platta nappe mark the oceanic suture between Margna-Sella fragment and Austroalpine mainland. Col-





lison and suturing occurred already in the Cretaceous, as indicated by the following facts: (1) The Margna-Platta boundary is truncated by the Corvatsch mylonite zone, a Late Cretaceous extensional fault (Liniger 1992; our Fig. 15b). (2) The Platta-Err boundary is folded around a fold of the Ducan-Ela phase, also Late Cretaceous in age (Fig. 3a).

Stretching lineations and shear sense determinations related to the Trupchun phase are represented in Figure 15a. Top-northwest to top-west thrusting prevails, and even top-southwest directed thrusting is documented from the area of the Margna nappe (Liniger 1992). The thrust geometry was largely influenced by the inherited geometry of the Jurassic passive continental margin (Fig. 1b). The latter was characterized by two systems of normal faults, an east-dipping system in the eastern, proximal part and a west-dipping system in the western, distal part (Froitzheim & Eberli 1990). An outer basement high had formed between the west-dipping and the east-dipping fault system, in the area that later became the Bernina nappe. The Jurassic to Lower Cretaceous sedimentary cover of this area is in places extremely thin and reflects erosion and condensed sedimentation on a submarine high (e. g. in the Schlattain-Clavadatsch unit of the Samedan zone, Rösli 1946).

Fig. 15. Maps showing orientation of structures related to different deformation phases in the Austroalpine of Graubünden. For locations compare Fig. 1.

(a) Early, thrusting-related structures of the Trupchun phase. Shear sense of mylonites yields consistently northwest- to west-directed transport. Southwest-directed shearing occurred in the Margna nappe and its vicinity (SW part of map, data from Liniger 1992). The Albula steep zone (vertical ruling) is interpreted as a zone of sinistral shearing also formed in the Trupchun phase. Front of main Upper Austroalpine basement sheets (Campo and Silvretta) is displaced across Albula steep zone.

(b) Late Cretaceous normal faults, mostly low-angle, of the Ducan-Ela phase. Arrows indicate transport direction of respective hanging walls, as derived from kinematic analysis of mylonites and cataclasites (partly data from Liniger 1992, Weh 1992, Spillmann 1993). CBF, Corvatsch-Bernina boundary fault (Fuorcla Surlej – Val Roseg – Fuorcla da la Sella); CMZ, Corvatsch mylonite zone; DNF, Ducan normal fault; JBF, base of the Julier nappe (prolongation of CBF northwest of the Engadine line); MNF, Mezzaun normal fault, between Seja basement below and Mezzaun sediments above; RNF, Rothorn normal fault, between Rothorn nappe below and Arosa Dolomites above; TNF, Trupchun normal fault, between Murtiröl unit below and Ortler nappe above (compare Fig. 5b in Schmid & Froitzheim 1993). Extension-related recumbent folding occurs in the footwall of a system of low-angle normal faults defined by the DNF, TNF, MNF and JBF.

(c) Early Tertiary folding (Blaisun phase) and northward thrusting of the orogenic lid comprising Austroalpine and Platta nappe. Fold axis orientations include data from Liniger (1992) and Handy et al. (1993). Latest Paleocene to Middle Eocene fossils at locality 1 (Parsonz flysch, Ziegler 1956, Eiermann 1988) and Middle Paleocene to Lower Eocene fossils at locality 2 (Tasna flysch, Rudolph 1982) indicate that thrusting of the orogenic lid over these units is post-Paleocene. Transport direction of the basal thrust (arrows) is derived from foliated cataclasites. Dashed parts of the basal thrust are overprinted by later faulting (Engadine line and Turba mylonite zone). A: northernmost possible position of the Austroalpine thrust front in the Late Paleocene to early Eocene; B: present Austroalpine front. These data require 75 km post-Paleocene northward thrusting.

(d) Postcollisional structures of Turba phase and Domleschg phase. The east-dipping Turba mylonite zone records east-directed downfaulting of the orogenic lid before intrusion of the Bergell granodiorite at 30 Ma. Note that the Turba m. z. is truncated by the Bergell intrusion on the southeast side of the Engadine line. East- to northeast-trending Domleschg-phase folds are younger than the Turba mylonite zone. Engadine line and Insubric line are conjugate faults accommodating eastward extrusion of the intervening block. Vertical displacement (“+” and “-” symbols) changes along the Engadine line and is zero at neutral point between St. Moritz and Samedan.

In the proximal part of the margin, especially in the Ortler zone, east-dipping high-angle Jurassic normal faults were transported within thrust sheets and were thus preserved almost in their original configuration (Froitzheim 1988), or were reactivated as thrusts (Manatschal 1991, Conti et al. 1994). The outer basement high was transformed into the Bernina nappe. The basement-dominated character of this nappe, with massive basement sheets and thin cover synclines, is directly inherited from its position in the passive margin. The sediment fill of normal-fault-bounded half grabens immediately east of the basement high partly remained in place, that is, connected to the basement of the Bernina nappe (Piz Alv, Sassalbo, Mezzaun, Pl. 1), partly was sheared off and transported to the west, over the basement culmination, as in the case of the Ela nappe. The pronounced stretching lineation ubiquitous in the Jurassic rocks of the Ela nappe may result from this special situation: These sedimentary rocks were “rolled out” between the obstacle of the Bernina basement below and the Upper Austroalpine basement above (Silvretta, Languard, Campo). In the Err nappe, west of the basement high, Jurassic normal faults were again partly preserved and only weakly overprinted by Alpine deformation (Froitzheim & Eberli 1990). This may be explained by the “pressure shadow” of the Bernina basement high, and by the westward dip of Jurassic normal faults in the Err nappe, unsuitably oriented for reactivation in a framework of top-west thrusting.

6.1.2 Sinistral wrench movement along the Albula steep zone

As stated above, Cretaceous orogeny in the western Austroalpine was dominated by top-west directed nappe imbrication. What is the role of the Albula steep zone in this context? This zone represents a lateral discontinuity of the nappe stack. It formed concomitant with nappe imbrication, or possibly, during a late stage of this imbrication. The significance of this zone may be understood by looking at the position of the crustal segments to the north and to the south of it in terms of Jurassic paleogeography. Across the Albula steep zone, the Upper Austroalpine Silvretta nappe to the north is laterally juxtaposed with the Lower Austroalpine Err-Carungas nappe to the south. The Err-Carungas nappe represents the most oceanward, western part of the Jurassic passive continental margin. In contrast, the Arosa Dolomites, today located at the western rim of the Silvretta nappe, represent a relatively proximal, continentward part of the passive margin (Furrer 1993, Eberli 1988). Therefore we interpret the Albula steep zone as a sinistral wrench zone along which Silvretta nappe and Arosa Dolomites moved from east to west relative to the Err nappe and other units to the south.

Figure 16 is a schematic reconstruction of the nappe geometry after the Trupchun phase. Platta-, Err-Carungas-, Ela-Bernina and Silvretta-Campo nappes had been imbricated along east-dipping thrusts. The Albula steep zone acted as a sinistral wrench zone within the nappe stack, accommodating different amounts of westward thrusting of Austroalpine units situated north and south of it. A northern block, including the Silvretta nappe, differentially advanced towards the west in respect to a southern block, including the Err nappe. This explains the counterclockwise rotation of D_1 folds in the Ela nappe and at the southwestern termination of the Ducan syncline. Slightly younger, upright D_1 folds in the Albula steep zone indicate a component of north-south shortening acting contemporaneously with sinistral wrench movement.

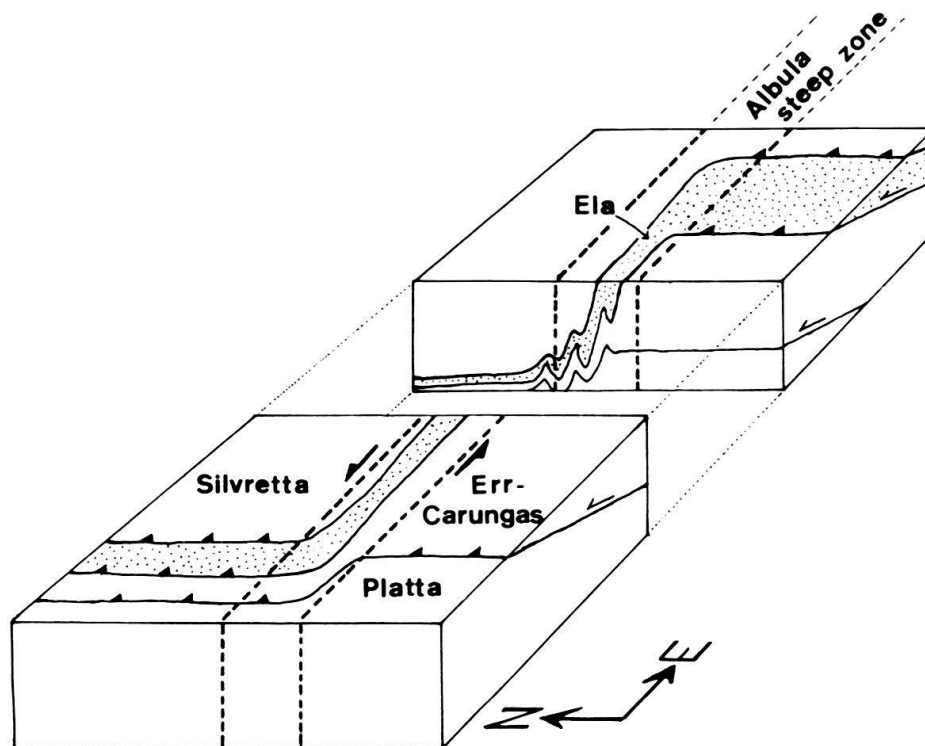


Fig. 16. Reconstruction of the "Albula steep zone". The Silvretta nappe advanced towards west relative to the Lower Austroalpine nappes (Ela, Err-Carungas) along an east-west trending, sinistral shear zone. Already existing thrusts were folded due to a component of north-south shortening concomitant with sinistral shearing in a late stage of the Trupchun phase (Late Cretaceous), leading to the steep orientation of the nappe boundaries.

The location of the eastern continuation of the Albula steep zone across the Engadine line remains uncertain, partly because of a severe extensional overprint in the Murtiröl-Mezzaun half window (Figs. 1, 15b). Retro-deformation of movements along the Engadine line (Schmid & Froitzheim 1993) constrains this continuation to be situated between the Campo basement to the south and the Sesvenna basement to the north. This can be used for an estimate of the displacement along the Albula steep zone. As discussed above, the Campo nappe and the Silvretta nappe occupy the same structural level in the original nappe pile. We assume that Campo and Silvretta were parts of one continuous basement complex before the displacement along the Albula steep zone. Today, the western boundary of the Silvretta basement and the western boundary of the Campo basement are offset in a sinistral sense by 40 to 45 km (Fig. 15a). Both boundaries are not erosional, in which case they could not be used for an estimation of the offset, but represent the primary front of the basement: the western front of the Campo basement is defined by the wedging-out of this unit between the underlying Languard nappe and the overlying Ortler nappe (Fig. 1), and the western front of the Silvretta basement is represented by a fold core enveloped by Permo-Triassic cover rocks. Therefore, this offset of 40 to 45 km constrains the displacement across the Albula steep zone. An independent estimate is provided by pronounced facies analogies in the Late Triassic and Early Jurassic of the Arosa Dolomites and the central Ortler nappe (Furrer 1993, Eberli 1988), indicating that these units are derived from closely neighbouring areas. The sinistral displace-

ment between these areas amounts to about 50 kilometres. This second estimate depends, of course, on a simple and possibly unrealistic arrangement of facies zones.

Late Cretaceous, east- to northeast-striking sinistral wrench faults in the Austroalpine realm were inferred on the grounds of paleogeographic considerations by Trümpy (1976). The Albula steep zone might well represent one of these. Another sinistral wrench zone was inferred between the Northern Calcareous Alps and the Central Austroalpine (Bechstädt 1978, Trümpy 1992), in order to account for the different facies of the Triassic in these two areas. In our study area, this other wrench zone would be situated between the Silvretta nappe to the south and the Northern Calcareous Alps to the north. This proposition is in good accordance with our observations. The Late Cretaceous to Eocene dextral movement in the Albula-Ortler zone proposed by Laubscher (1991), however, is in contradiction to the field evidence and has to be rejected. In our study area, we did not find any indication for dextral wrenching along east-striking faults or shear zones during the Cretaceous. The absence of such structures is remarkable, because dextral transpression was inferred as the general mechanism of Cretaceous deformation in the Austroalpine by many authors (Ratschbacher 1986, Ring et al. 1989, Ratschbacher et al. 1989, etc.).

6.1.3 Late Cretaceous extension: Collapse behind a migrating orogenic wedge

As demonstrated above for the Ducan normal fault and its continuation along the base of the Silvretta nappe, kinematic analysis of mylonitic and cataclastic fault rocks along shallowly dipping tectonic contacts has revealed important top-to-the-east extensional faulting in the Austroalpine units of Graubünden. Indicated in Figure 15b are normal faults that are ascribed to the Late Cretaceous extension, and shear direction and sense of associated fault rocks. Because the extensional faulting overprinted an earlier stack of nappes, normal faults do not always emplace younger rocks on older rocks, but the opposite is also observed.

The Trupchun normal fault (TNF) is interpreted as the continuation of the Ducan normal fault east of the Engadine line. Along this fault, the Upper Austroalpine Ortler nappe is directly emplaced on Cretaceous flysch of the Err system, and substantial parts of the nappe pile are omitted (Bernina nappe and Languard nappe). We have no fault rock data from this poorly exposed fault. The Mezzaun normal fault (MNF) forms the boundary between the Mezzaun sediments (Bernina system) above and the Seja basement and Murtiröl sediments (Err system) below. It represents a marked discontinuity crosscutting older structures. Scarce kinematic indicators from the main fault plane and its immediate vicinity (fibre-growth slickensides, grooves and ridges) indicate top-south-east directed movement. In contrast, paleostress analysis using minor faults in sedimentary rocks above the fault indicates top-southwest directed normal faulting (Schmid & Froitzheim 1993). In spite of this ambiguity concerning the exact movement direction, the normal-fault character of the MNF is clear because higher thrust sheets are emplaced on lower ones along this post-nappe discontinuity.

The Corvatsch-Bernina boundary fault (CBF) is a low-temperature quartz mylonite zone with top-east shear sense (Spillmann 1993). It partly coincides with an extremely thinned sediment syncline between two basement sheets, the Bernina nappe s. s. above and the Corvatsch nappe below. The Julier base fault (JBF) is the continuation of the

CBF north of the Engadine line. It represents an original thrust that was reactivated as a normal fault (Handy et al. 1993). The Corvatsch mylonite zone (CMZ) is a broad zone of basement- and sediment-derived mylonites between the Covatsch nappe above and the Platta nappe below. The shear sense is top-to-the-east (Müller 1982, Liniger 1992).

Another low-angle normal fault, the Peio line, is found outside our study area at the southeastern border of the Campo nappe (Werling 1992). This is an oblique-slip, top-east normal fault between two basement units of the Austroalpine, the Campo nappe below and the Tonale series above. The fault was active while greenschist facies conditions prevailed in the footwall (Werling 1992). The same author assumed a Late Cretaceous age for the activity of this normal fault.

Ducan-Ela-phase folds are most pronounced in the Lower Austroalpine west of and below a belt of normal faults defined by the DNF, TNF, MNF, CBF, CMZ and JBF (folded area indicated by oblique hatching in Fig. 15b). These folds reflect ductile stretching and vertical shortening of initially non-horizontal layers. Therefore the belt of normal faults is interpreted as a decoupling horizon between ductile extended crust below and brittlely extended crust above (Fig. 12).

The age of the Ducan-Ela phase was determined radiometrically by Tietz et al. (1993) on rocks from the Samedan zone: K-Ar dating on white mica grown along S_2 (Ducan-Ela phase) cleavage surfaces yielded ages of 67.5 ± 2.0 Ma, 79.7 ± 2.4 Ma, and 70.3 ± 0.3 Ma (Fig. 14). Late Cretaceous extension was also observed farther east in the Austroalpine (Ratschbacher et al. 1989). According to these authors, the formation of the Gosau sedimentary basins with 90 to 60 Ma old sediments was related to this extension. The rapid deepening of the basins at about 80 Ma is interpreted as marking the main extensional phase. Consequently, the extension began at 90 Ma east of the Tauern window. At this time, west-directed thrusting and folding of the Trupchun phase just began in the Austroalpine of Graubünden (see above). This indicates a westward migration of both crustal shortening and immediately following east-west extension, as already assumed by Ratschbacher et al. (1989). Such a scenario is compatible with the westward progradation of the orogenic wedge system. In this case, Gosau and Ducan-Ela extension could be caused by an overthickened wedge according to the model of Platt (1986), migrating towards the west.

The westward migration of the orogenic wedge has an important implication: It becomes unlikely that the subduction of South Penninic oceanic lithosphere under the Apulian plate represents the "motor" for Cretaceous orogeny in the Austroalpine. If Cretaceous orogeny had been caused by this subduction, thrusting should have occurred first in the distal continental margin, that is, in the Lower Austroalpine. This is not the case. Instead, the thrusting started in the internal parts of the Austroalpine and reached the ocean-continent transition only at a late stage. Consequently, the formation of the Austroalpine orogenic wedge is better explained by a continental collision east or southeast of the Austroalpine realm, i. e. along the Vardar-Hallstatt ocean, as proposed by Thöni & Jagoutz (1993).

6.2 Tertiary orogeny

6.2.1 Early Tertiary collisional deformation

After the Late Cretaceous extensional phase, the Austroalpine – Upper Penninic nappe edifice was thrust as a “*traîneau écraseur*” (Termier 1903) or “*orogenic lid*” (Laubscher 1983) towards north over the Middle and North Penninic units. The basal thrust of the orogenic lid is exposed at the western border of the Engadine window, between basement rocks of the Silvretta nappe above and Mesozoic sediments of the Arosa zone below (Laubscher 1983). This thrust is of Tertiary age, because it truncates pseudotachylite veins which yielded Late Cretaceous ages (78.5+4.6 Ma and 73.2+3.2 Ma, Rb-Sr thin slab isochrons, Thöni 1988) and are in our opinion related to crustal extension during the Duncan-Ela phase (Fig. 14). Shear-sense indicators in a thin mylonite layer along the thrust give top-north-directed movement (arrows in Fig. 15c). Late, top-north directed movement following earlier, west-directed shearing was also demonstrated for the Arosa zone along the western margin of the Austroalpine and in the Engadine window by Ring et al. (1988, 1989). The north- to slightly north-northeastward transport direction (Fig. 15c, see also Ring et al. 1988, 1989) differs from the northwest to north-northwest directed transport inferred for the same time interval in the Penninic Schams nappes (F_1 of Schmid et al. 1990). The Schams nappes, however, are severely overprinted by later deformation. Hence we regard the kinematic data presented in Figure 15c to be more reliable.

The southward continuation of the Tertiary-age basal thrust at the western margin of the Austroalpine units must be assumed beneath the Platta nappe, because Platta and Margna nappes were welded to the Austroalpine already in the Cretaceous (see above). Both Platta nappe and Margna nappe were part of the orogenic lid in the Tertiary (Liniger & Nievergelt 1990). This implies that the tectonic position of the Platta nappe is fundamentally different from that of the Arosa zone, although both units comprise ophiolites of the South Penninic ocean: the Arosa zone is a *mélange* between ophiolites and Austroalpine units that formed during Cretaceous subduction and was reworked in Tertiary time as a top-north directed shear zone below the orogenic lid. The Platta nappe, however, represents ophiolites which were accreted to the Austroalpine continental margin in the Cretaceous and became part of the orogenic lid in the Tertiary. The base of the Platta nappe was overprinted by the Turba mylonite zone later on during the Early Oligocene. Therefore, the basal thrust of the Tertiary-age orogenic lid is not preserved in the Oberhalbstein area and south of it (dashed continuation of the thrust in SW part of Fig. 15c).

The grade of the Late Cretaceous metamorphism in the units overlying the basal thrust of the Tertiary-age orogenic lid decreases from south to north, from the higher greenschist facies in the Margna nappe (Guntli & Liniger 1989) to the diagenesis/anchizone boundary at the western border of the Silvretta nappe (Dunoyer de Segonzac & Bernoulli 1976). Consequently, the southernmost units forming the orogenic lid were detached from deeper parts of the crust in the Early Tertiary. This geometry explains the strong reduction or total lack of Lower Austroalpine units in the north, that is, in the Engadine window and in the Prättigau half-window (Fig. 1). The basal thrust of the Tertiary orogenic lid must have climbed into increasingly higher previously emplaced, i. e. Cretaceous, nappe units from south to north.

Tertiary fossils were found in flysch sediments below the orogenic lid in the Oberhalbstein area (Ziegler 1956) and in the Engadine window (Rudolph 1982), indicating

that Tertiary thrusting is post-Paleocene (Fig. 14). The foraminifera in the Oberhalbstein are Latest Paleocene to Middle Eocene (Eiermann 1988) corresponding to about 57 Ma to 38.6 Ma (Harland et al. 1990). The ones in the Tasna flysch of the Engadine window are Middle Paleocene to Early Eocene (Rudolph 1982), corresponding to 60.5 to 50 Ma. These findings allow an estimate for the amount of thrusting during the Tertiary. To allow for the sedimentation of the Tertiary flysch in the Oberhalbstein area, the front of the Austroalpine must still have been south of this area in the Early Eocene. Today, this front is at the northern border of the Alps. These constraints indicate a Tertiary northward displacement of the orogenic lid of at least 75 km, measured parallel to the movement direction (north).

The orogenic lid was not an absolutely rigid block, but suffered some internal deformation: it was affected by east- to southeast-trending folds of the Blaisun phase (Fig. 15c). The exact relative timing of northward thrusting and Blaisun-phase folding in the Austroalpine is not known. We assume, however, that both phenomena were closely related, if not coeval. The strike of Blaisun-phase folds is relatively uniform, southeast to east and thus roughly perpendicular to the transport direction of the basal thrust of the orogenic lid (Fig. 15c). The dip of axial planes, however, is variable: At the southern border of the Silvretta nappe, axial planes are subvertical, steeply north-dipping, or steeply south-dipping (e. g. Fig. 3b). In the Ortler nappe, axial surfaces dip south (Conti et al. 1994). In the southern part of the Austroalpine, e. g. in the Malenco area, the axial surfaces of the Blaisun phase are generally N-dipping ("First phase of backfolding", Hermann & Müntener 1992). This is also the case at the western border of the Err-Carungas nappe (Dürr 1992). This variability and the lack of a predominant vergence indicate that Blaisun-phase folding reflects inhomogeneous internal shortening of the orogenic lid. On a very large scale, this internal shortening was near-coaxial.

Northward thrusting of the orogenic lid and Blaisun-phase folding are probably related to the continental collision that occurred after subduction of the last remaining oceanic lithosphere, the Valais ocean, at about 40 Ma (Frisch 1979). The change from Cretaceous westward thrusting to Early Tertiary northward thrusting is not a gradual one. Instead, Cretaceous and Tertiary thrusting are clearly separated by the Late Cretaceous extensional event. After the extensional event, renewed thrusting began with a N-directed transport direction, almost perpendicular to the Cretaceous shortening.

6.2.2 Postcollisional deformation of the Austroalpine nappes

Tertiary northward thrusting and folding during the Blaisun phase were followed by renewed east-west extension during the Turba phase. Liniger (1992) showed that the Turba mylonite zone is intruded by the Bergell granodiorite (30 Ma, von Blanckenburg 1992). On the other hand, the mylonite zone affects the Arblatsch flysch, deposited until about 50 Ma (Early to Middle Eocene, Ziegler 1956). Thus, the Turba mylonite zone must have formed between about 50 and 30 Ma. Because the northward thrusting of the orogenic lid over the Lower and Middle Penninic units predates the Turba extension, we place the Turba phase towards the end of this time span, that is, in the Early Oligocene (Fig. 14).

Extensional faulting along the Turba mylonite zone is intimately linked to recumbent folding in the footwall of this zone, i. e. in the Suretta and Schams nappes and surrounding units (Niemet-Beverin phase, D₂ of Schmid et al. 1990 and Schreurs 1993). Folding of

the Niemet-Beverin phase is viewed in the context of vertical extrusion from an east-west-striking zone immediately north of the Insubric Line (Schmid et al. 1990, Merle & Guillier 1989). According to new data, this Niemet-Beverin-phase folding was accompanied by east-west extension and vertical shortening (Baudin et al. 1993, Nievergelt et al. in press). The Turba mylonite zone marks a final stage of this extension. These relations indicate that the east-west directed Turba extension was roughly contemporaneous with north-south shortening. Therefore the Turba extension is not regarded as a postorogenic collapse leading to crustal thinning.

A second step of postcollisional deformation is represented by the folds of the Domleschg phase and by the movements along the Engadine line (Fig. 15d). The Domleschg phase is probably pre-Miocene: cooling through 300 °C near the Oligocene-Miocene boundary is reported for the southern Tambo nappe (Jäger et al. 1967, Purdy & Jäger 1976), a region affected by Domleschg-phase folding (F_3 of Baudin et al. 1993). The ductile style of Domleschg-phase folding in this area requires temperatures above 300 °C. This suggests that Domleschg-phase folding occurred before or near the Oligocene-Miocene boundary.

In the Suretta and Tambo nappes and surrounding units, west and northwest of the Bergell intrusion, the Domleschg-phase folds exhibit a general vergence towards north, with steeply southeast- to south-dipping axial surfaces (F_3 of Schmid et al. 1990, Baudin et al. 1993). The northeastward trend of fold axes, indicating southeast-northwest directed shortening, is in accordance with a framework of dextral transpression along the Insubric line. In fact, the timing of the Domleschg phase coincides with the beginning of the "Insubric phase" of dextral transpression in the Late Oligocene (Schmid et al. 1987). Hence the kinematic framework of NW-SE directed shortening, typical for the external zones of the Alps, was not established until the Late Oligocene.

Field relations in the upper Val Bregaglia suggest that the Engadine line postdates the Domleschg phase: the style of Domleschg-phase folds is ductile in this area, whereas deformation along the Engadine line is brittle. According to the kinematic analysis of Schmid & Froitzheim (1993), movement along the Engadine line was a combination of sinistral strike-slip and block rotation. Along the southwestern part of the line, the block rotation resulted in relative uplift of the southeastern block. To the northeast, the vertical component was reversed and the northwestern block was uplifted relatively. A neutral point with no vertical displacement exists between St. Moritz and Samedan. There, the displacement is sinistral strike-slip on the order of 3 km.

In the area of Maloja pass, near the northern end of the Bergell intrusion, the Engadine line truncates the contact metamorphic aureole of the intrusion (Fig. 4 in Trommsdorff & Nievergelt 1983). The relative uplift of the Bergell intrusion caused by movements along the Engadine line is very substantial and amounts to 7 km along the profile on the front of the block diagram in Plate 1. The counterpart of the relative uplift of the Bergell intrusion and its countryrocks along the southwestern Engadine line, is the exhumation of the Engadine window in the Lower Engadine, situated along the northeastern part of this line (Pl. 1). In the vicinity of the Engadine window, the Engadine line dips southeast and acted as a major oblique-slip normal fault with a vertical displacement component of at least 3 kilometres, downthrowing the southeastern block relative to the northwestern block (Schmid & Haas 1989, Schmid & Froitzheim 1993). The Engadine window is situated on the uplifted shoulder of the northwestern block. Additionally, the

window is accentuated by a major northeast-striking antiform which we correlate with the Domleschg phase. The hinge of this antiform is near the southeastern border of the window (Fig. 15d; Gürler 1982).

According to a fault plane analysis along the Engadine line (Schmid & Froitzheim 1993), the least compressive principal stress (σ_3) was constantly oriented E-W all along the Engadine line, suggesting that an east-west stretch was accommodated by a combination of normal faulting and sinistral strike-slip movement. The sinistral movement along the Engadine line and the dextral movement along the Insubric line accommodated eastward extrusion (in the sense of Ratschbacher et al. 1991) of the triangular block bounded by these two lines (Fig. 15d), leading to local east-west directed extension also during this stage. Late Miocene deformation in the Southern Alps and along the Giudicarie line postdates this east-west stretch (Schmid & Froitzheim 1993). Therefore a Latest Oligocene to Early Miocene age is inferred for the movements along the Engadine line.

7 Conclusions

Two orogenic cycles, of Cretaceous and Tertiary age, have been demonstrated by the structural analysis of the Austroalpine nappes in Graubünden. The first cycle included west- to northwestward imbrication of upper crustal thrust sheets and sinistral transpression along the east-striking Albula steep zone (Trupchun phase), followed by east-southeast directed extensional overprint of the nappe edifice, involving low-angle normal faults and recumbent "collapse folds" (Ducan-Ela phase). In the second cycle, of Tertiary age, the Austroalpine and previously accreted Upper Penninic units were thrust northward and emplaced as an orogenic lid on the deeper Penninic units. Internal folding of the orogenic lid was associated with this northward thrusting (Blaisun phase, Eocene). Thrusting and folding were followed by a second phase of east-west extension, roughly contemporaneous with ongoing north-south compression (Turba phase, Early Oligocene). This second extensional event was followed by NW-SE shortening (Domleschg phase, Late Oligocene), and by sinistral slip and block rotation along the Engadine line near the Oligocene-Miocene boundary.

Regarding the Cretaceous orogeny in the Austroalpine realm, the following inferences can be drawn: (1) Cretaceous crustal shortening was accommodated by top-west to top-northwest thrusting. On the scale of the entire Austroalpine realm, this shortening propagated from east to west and was followed by an extensional collapse, also propagating from east to west. The westward migration of the orogenic wedge implies that Cretaceous orogeny did not result from the subduction of South Penninic oceanic lithosphere under the Austroalpine realm, but rather from a collision event east or southeast of the Austroalpine realm. (2) In the study area, we found no indications for Cretaceous dextral wrench movements as expected from broadly accepted models which assume a dextrally transpressive framework for the Cretaceous orogeny (Ratschbacher 1986, Ring et al. 1989, Ratschbacher et al. 1989). On the contrary, a sinistrally transpressive shear zone is observed (Albula steep zone), in accordance with models of Trümpy (1976) and Bechstädt (1978).

The recognition of two orogenic cycles contradicts the classical view of the Alpine orogeny as a continuous tectonometamorphic evolution. This view regarded all high-pressure metamorphism, even in the Penninic units, to be of Cretaceous age. Since our

data indicate two cycles of crustal shortening followed by exhumation, they lend additional support for models postulating a second period of subduction in the Tertiary, leading to the closure of the North Penninic ocean (Schmid et al. 1990, Gebauer et al. 1992, Becker 1993). Our reconstruction of the tectonic evolution suggests that the high-pressure metamorphism within northern parts of the Penninic zone, e. g. in the Dora Maira massif, the Adula nappe, and the Tauern window, may be of Tertiary age.

Acknowledgments

This work was supported by Swiss National Science Foundation grants 21-25252.88 and 20-29869.90, and by the Deutsche Forschungsgemeinschaft grant Fr 700/1-1. We thank G. Eberli, U. Eichenberger, H. Furrer, M. Handy, G. Manatschal, P. Nievergelt and M. Weh for stimulating discussions. Reviews by G. Eberli, W. Frisch and M. Handy helped to improve a first version of this paper. We dedicate the present article to Rudolf Trümpy for two reasons. Firstly, this work would not have been possible without the solid stratigraphic-sedimentological framework layed out by his research group at ETH. Secondly, he has been a constant source of inspiration also concerning tectonic interpretations. We benefited from many discussions with him, both in the field and in the laboratory.

REFERENCES

- BAUDIN, T., MARQUER, D. & PERSOZ, F. 1993: Basement-cover relationships in the Tambo nappe (Central Alps, Switzerland): geometry, structure and kinematics. *J. struct. geol.* 15, 543–553.
- BEARTH, P., EUGSTER, H., SPAENHAUER, F., STRECKEISEN, A. & LEUPOLD, W. 1935: Geologischer Atlas der Schweiz 1:25 000, Blatt 9: Scalettapass. Schweiz. geol. Komm.
- BECHSTÄDT, T. 1978: Faziesanalyse permischer und triadischer Sedimente des Drauzuges als Hinweis auf eine grossräumige Lateralverschiebung innerhalb des Ostalpins. *Jb. geol. Bundesanst. (Wien)*121, 1–121.
- BECKER, H. 1993: Garnet peridotite and eclogite Sm-Nd mineral ages from the Lepontine dome (Swiss Alps): New evidence for Eocene high-pressure metamorphism in the central Alps. *Geology* 21, 599–602.
- BLANCKENBURG, VON, F. 1992: Combined high-precision chronometry and geochemical tracing using accessory minerals: applied to the Central-Alpine Bergell intrusion (central Europe). *Chem. Geol.* 100, 19–40.
- BRAUCHLI, R. 1921: Geologie der Lenzerhorngruppe. *Beitr. geol. Karte Schweiz N.F.* 49/2, 1–106.
- BRAUCHLI, R. & GLASER, T. 1922: Geologische Karte von Mittelbünden 1:25 000, Blatt Lenzerhorn. Spezialkarte 94C, Schweiz. Geol. Komm.
- CARON, M., DÖSEGGER, R., STEIGER, R. & TRÜMPY, R. 1982: Das Alter der jüngsten Sedimente der Ortler-Decke (Oberostalpin) in der Val Trupchun (Schweizerischer Nationalpark, Graubünden). *Eclogae geol. Helv.* 75, 159–169.
- CONTI, P. 1992: Tettonica delle falde Austroalpine nelle dolomite dell'Engadina: un'ipotesi di Lavoro. *Atti Tic. Sc. Terra* 35, 61–66.
- CONTI, P., MANATSCHAL, G. & PFISTER, M. 1994: Synrift sedimentation, Jurassic and Alpine tectonics in the central Ortler nappe (Eastern Alps, Italy). *Eclogae geol. Helv.* 87, 63–90.
- CORNELIUS, H.P. 1932: Geologische Karte der Err-Julier-Gruppe 1:25 000, Ost- und Westblatt. Spezialkarte 115, Schweiz. Geol. Komm.
- 1935: Geologie der Err-Julier-Gruppe: Das Baumaterial. *Beitr. geol. Karte Schweiz N.F.* 70/1, 1–321.
- 1950: Geologie der Err-Julier-Gruppe: Der Gebirgsbau. *Beitr. geol. Karte Schweiz N.F.* 70/2, 1–264.
- DAL PIAZ, G.V., DEL MORO, A., MARTIN, S. & VENTURELLI, G. 1988: Post-collisional magmatism in the Ortler-Cevedale Massif (Northern Italy). *Jb. geol. Bundesanst. (Wien)*131, 533–551.
- DUNOYER DE SEGONZAC, G. & BERNOULLI, D. 1976: Diagenèse et métamorphisme des argiles dans le Rhétien Sud-alpin et Austro-alpin (Lombardie et Grisons). *Bull. Soc. géol. France* 18, 1283–1293.
- DÜRR, S.B. 1992: Structural history of the Arosa zone between Platta and Err nappes east of Marmorera (Grisons): Multi-phase deformation at the Penninic-Austroalpine plate boundary. *Eclogae geol. Helv.* 85, 361–374.
- EBERLI, G.P. 1985: Die jurassischen Sedimente in den ostalpinen Decken Gaubündens – Relikte eines passiven Kontinentalrandes. *Diss. ETH Zürich* Nr. 7835.

- 1988: The evolution of the southern continental margin of the Jurassic Tethys Ocean as recorded in the Allgäu Formation of the Austroalpine Nappes of Graubünden (Switzerland). *Eclogae geol. Helv.* 81, 175–214.
- EGGENBERGER, H. 1926: Geologie der Albulazone zwischen Albulahospiz und Scans (Graubünden). *Eclogae geol. Helv.* 19, 523–571.
- EICHENBERGER, U. 1986: Die Mitteltrias der Silvretta-Decke (Ducankette und Landwassertal, Ostalpin). *Mitt. Geol. Inst. Univ. u. ETH Zürich N.F.* 252, 1–196.
- EIERMANN, D.R. 1988: Zur Stellung des Martegnas-Zuges. *Eclogae geol. Helv.* 81, 259–272.
- EUGSTER, H. 1923: Geologie der Ducangruppe. *Beitr. geol. Karte Schweiz N.F.* 49/3, 1–134.
- 1924: Die westliche Piz Uertsch-Kette (Preda-Albulapass): *Beitr. geol. Karte Schweiz N.F.* 49/4, 1–31.
- EUGSTER, H. & FREI, F. 1927: Geologische Karte von Mittelbünden 1:25 000, Blatt Bergün. Spezialkarte 94F, Schweiz. Geol. Komm.
- EUGSTER, H. & LEUPOLD, W. 1930: Geologische Karte von Mittelbünden 1:25 000, Blatt Landwasser. Spezialkarte 94D, Schweiz. Geol. Komm.
- FREI, F. 1925: Geologie der östlichen Bergünstöcke (Piz d'Aela und Tinzenhorn, Graubünden). *Beitr. geol. Karte Schweiz N. F.* 49/6, 1–30.
- FREI, F. & OTT, E. 1926: Geologische Karte von Mittelbünden 1:25 000, Blatt Piz Michèl. Spezialkarte 94E, Schweiz. Geol. Komm.
- FRISCH, W. 1979: Tectonic progradation and plate tectonic evolution of the Alps. *Tectonophysics* 60, 121–139.
- 1980: Plate motions in the Alpine region and their correlation to the opening of the Atlantic ocean. *Geol. Rdsch.* 70, 402–411.
- FROITZHEIM, N. 1988: Synsedimentary and synorogenic normal faults within a thrust sheet of the Eastern Alps (Ortler zone, Graubünden, Switzerland). *Eclogae geol. Helv.* 81, 593–610.
- 1992: Formation of recumbent folds during synorogenic crustal extension (Austroalpine nappes, Switzerland). *Geology* 20, 923–926.
- FROITZHEIM, N. & EBERLI, G. P. 1990: Extensional detachment faulting in the evolution of a Tethys passive continental margin, Eastern Alps, Switzerland. *Geol. Soc. Amer. Bull.* 102, 1297–1308.
- FURRER, H. 1993: Stratigraphie und Fazies der Trias/Jura-Grenzsichten in den Oberostalpinen Decken Graubündens. *Diss. Univ. Zürich.*
- FURRER, H., EICHENBERGER, U., FROITZHEIM, N. & WURSTER, D. 1992: Geologie, Stratigraphie und Fossilien der Ducankette und des Landwassergebiets (Silvretta-Decke, Ostalpin). *Eclogae geol. Helv.* 85, 245–256.
- GEBAUER, D., GRÜNENFELDER, M., TILTON, G., TROMMSDORFF, V. & SCHMID, S. 1992: The geodynamic evolution of garnet-peridotites, garnet-pyroxenites and eclogites of Alpe Arami and Cima di Gagnone (Central Alps) from Early Proterozoic to Oligocene. *Schweiz. mineral. petrogr. Mitt.* 72, 107–111.
- GUNTLI, P. & LINIGER, M. 1989: Metamorphose in der Margna-Decke im Bereich Piz da la Margna und Piz Fedoz (Oberengadin). *Schweiz. mineral. petrogr. Mitt.* 69, 289–301.
- GÜRLER, B. 1982: Geologie des Val Tasna und Umgebung (Unterengadin). *Diss. Univ. Basel.*
- HANDY, M. R., HERWEGH, M. & REGLI R. 1993: Tektonische Entwicklung der westlichen Zone von Samedan (Oberhalbstein, Graubünden, Schweiz). *Eclogae geol. Helv.* 86, 785–817.
- HARLAND, W. B., ARMSTRONG, L. R., COX, A. V., CRAIG, L. E., SMITH, A. G. & SMITH, D. G. 1990: A geologic time scale 1989. Cambridge University Press, Cambridge etc.
- HEIERLI, H. 1955: Geologische Untersuchungen in der Albulazone zwischen Crap Alv und Cinuos-chel (Graubünden). *Beitr. geol. Karte Schweiz N. F.* 101, 1–105.
- HEIM, A. 1922: Geologie der Schweiz. Band II: Die Schweizer Alpen. Tauchnitz, Leipzig.
- HERMANN, J. & MÜNTENER, O. 1992: Strukturelle Entwicklung im Grenzbereich zwischen dem penninischen Malenco-Ultramafitit und dem Unterostalpin (Margna- und Sella-Decke). *Schweiz. mineral. petrogr. Mitt.* 72, 225–240.
- JÄGER, E., NIGGLI, E. & WENK, E. 1967: Rb-Sr Altersbestimmungen an Glimmern der Zentralalpen. *Beitr. geol. Karte Schweiz, N. F.* 134.
- LAUBSCHER, H. P. 1983: Detachment, shear and compression in the Central Alps. *Geol. Soc. Amer. Mem.* 158, 191–211.
- 1991: The arc of the Western Alps today. *Eclogae geol. Helv.* 84, 631–659.
- LEMOINE, M., TRICART, P. & BOILLOT, G. 1987: Ultramafic and gabbroic ocean floor of the Ligurian Tethys (Alps, Corsica, Apennines): In search of a genetic model. *Geology* 15, 622–625.
- LINIGER, M. H. 1992: Der ostalpin-penninische Grenzbereich im Gebiet der nördlichen Margna-Decke (Graubünden, Schweiz). *Diss. ETH Zürich Nr.* 9769.

- LINIGER, M. H. & NIEVERGELT, P. 1990: Stockwerk-Tektonik im südlichen Graubünden. Schweiz. mineral. petrogr. Mitt. 70, 95–101.
- LOZZA, H. 1990: Stratigraphie und Tektonik der unterostalpinen Err- und Carungas-Einheiten in der Val d'Err (Oberhalbstein). Unpubl. diploma thesis, Geol. Inst. ETH and Univ. Zürich.
- MAGGETTI, M. & FLISCH, M. 1993: Evolution of the Silvretta nappe. In: Pre-Mesozoic geology in the Alps. (Ed. by Raumer, von, J. F. & Neubauer F.) Springer Verlag, Berlin/Heidelberg, 469–484.
- MANATSCHAL, G. 1991: Zur Geologie zwischen Monte Torracchia und Valle di Fraele (Ortler-Element). Unpubl. diploma thesis, Geol. Inst. ETH and Univ. Zürich.
- MERLE, O. & GUILLIER, B. 1989: The building of the central Swiss Alps: an experimental approach. Tectonophysics 165, 41–56.
- MÜLLER, D. 1982: Geologie und Petrographie der Bernina I. Kristallisation, Deformation und Geochemie des südlichen Corvatschgranits im Oberengadin GR. Unpubl. diploma thesis, Univ. Zürich.
- NAEF, H. 1987: Ein Beitrag zur Stratigraphie der Trias-Serien im Unterostalpin Graubündens (Grisoniden). Mitt. Geol. Inst. ETH u. Univ. Zürich N. F. 276, 1–206.
- NIEVERGELT, P., LINIGER, M., FROITZHEIM, N. & FERREIRO-MAEHLMANN R. 1991: The Turba mylonite zone: An Oligocene extensional fault at the Pennine-Austroalpine boundary in eastern Switzerland. Terra abstracts 3, 248.
- NIEVERGELT, P., LINIGER, M., FROITZHEIM, N. & FERREIRO-MAEHLMANN R. IN PRESS: Early to mid Tertiary crustal extension in the Central Alps. The Turba Mylonite Zone (Eastern Switzerland). Tectonics.
- ÖBERHAUSER, R. 1991: Westvergente versus nordvergente Tektonik – Ein Beitrag zur Geschichte und zum Stand geologischer Forschung, gesehen von der Ost-Westalpengrenze her. Jb. geol. Bundesanst. (Wien) 134, 773–782.
- OTT, E. 1925: Geologie der westlichen Berggünerstöcke (Piz Michèl und Piz Toissa, Graubünden). Beitr. geol. Karte Schweiz N. F. 49/5, 1–102.
- PIFFNER, O. A. 1977: Tektonische Untersuchungen im Infrahelvetikum der Ostschweiz. Diss. ETH Zürich Nr. 5911.
- PITTET, C. 1993: Geologie und Sedimentologie der ostalpinen Ela-Decke am Albulapass, Graubünden. Unpubl. diploma thesis, Univ. Basel.
- PLATT, J. P. 1986: Dynamics of orogenic wedges and the uplift of high-pressure metamorphic rocks. Bull. geol. Soc. Amer. 97, 1037–1053.
- PURDY, J. W. & JÄGER, E. 1976: K-Ar ages on rock-forming minerals from the Central Alps. Mem. Ist. Geol. Mineral. Univ. Padova 30, 1–30.
- RAMSAY, J. G. 1967: Folding and fracturing of rocks. McGraw-Hill, New York.
- RATSCHBACHER, L. 1986: Kinematics of Austro-Alpine cover nappes: Changing translation path due to transpression. Tectonophysics 125, 335–356.
- RATSCHBACHER, L., FRISCH, W., NEUBAUER, F., SCHMID, S. M. & NEUGEBAUER, J. 1989: Extension in compressional orogenic belts: The eastern Alps. Geology 17, 404–407.
- RATSCHBACHER, L., FRISCH, W., LINZER, G. & MERLE, O. 1991: Lateral extrusion in the Eastern Alps, part 2: Structural analysis. Tectonics 10/2, 257–271.
- RING, U., RATSCHBACHER, L. & FRISCH, W. 1988: Plate-boundary kinematics in the Alps: Motion in the Arosa Suture Zone. Geology 16, 696–698.
- RING, U., RATSCHBACHER, L., FRISCH, W., BIEHLER, D. & KRÁLIK, M. 1989: Kinematics of the Alpine plate-margin: structural styles, strain and motion along the Penninic-Austroalpine boundary in the Swiss-Austrian Alps. J. geol. Soc. (London) 146, 835–849.
- RING, U., RATSCHBACHER, L., FRISCH, W., DÜRR, S. & BORCHERT, S. 1990: The internal structure of the Arosa zone (Swiss-Austrian Alps). Geol. Rdsch. 79, 725–739.
- 1991: Late-stage east-directed deformation in the Platta, Arosa and lowermost Austroalpine nappes (eastern Swiss Alps). N. Jb. Geol. Paläont. (Mh.) 1991/6, 357–363.
- RÖSLI, F. 1927: Zur Geologie der Murtirölgruppe bei Zuoz (Engadin). Jb. Phil. Fak. II Univ. Bern 7, 140–156.
- 1946: Sedimentäre Zone von Samaden (Samaden Kt. Graubünden). Eclogae geol. Helv. 38, 329–336.
- ROTHPLETZ, A. 1905: Geologische Alpenforschungen II, Ausdehnung und Herkunft der Rhaetischen Schubmasse. Lindauer, München.
- RUDOLPH, J. 1982: Tieferes Tertiär im oberen Fimbartal, Unterengadiner Fenster. N. Jb. Geol. Paläont. (Mh.) 1982/3, 181–183.
- SCHMID, S. M. 1973: Geologie des Umbrailgebietes. Eclogae geol. Helv. 66, 101–210.
- SCHMID, S. M., ZINGG, A. & HANDY, M. 1987: The kinematics of movements along the Insubric Line and the emplacement of the Ivrea Zone. Tectonophysics 135, 47–66.

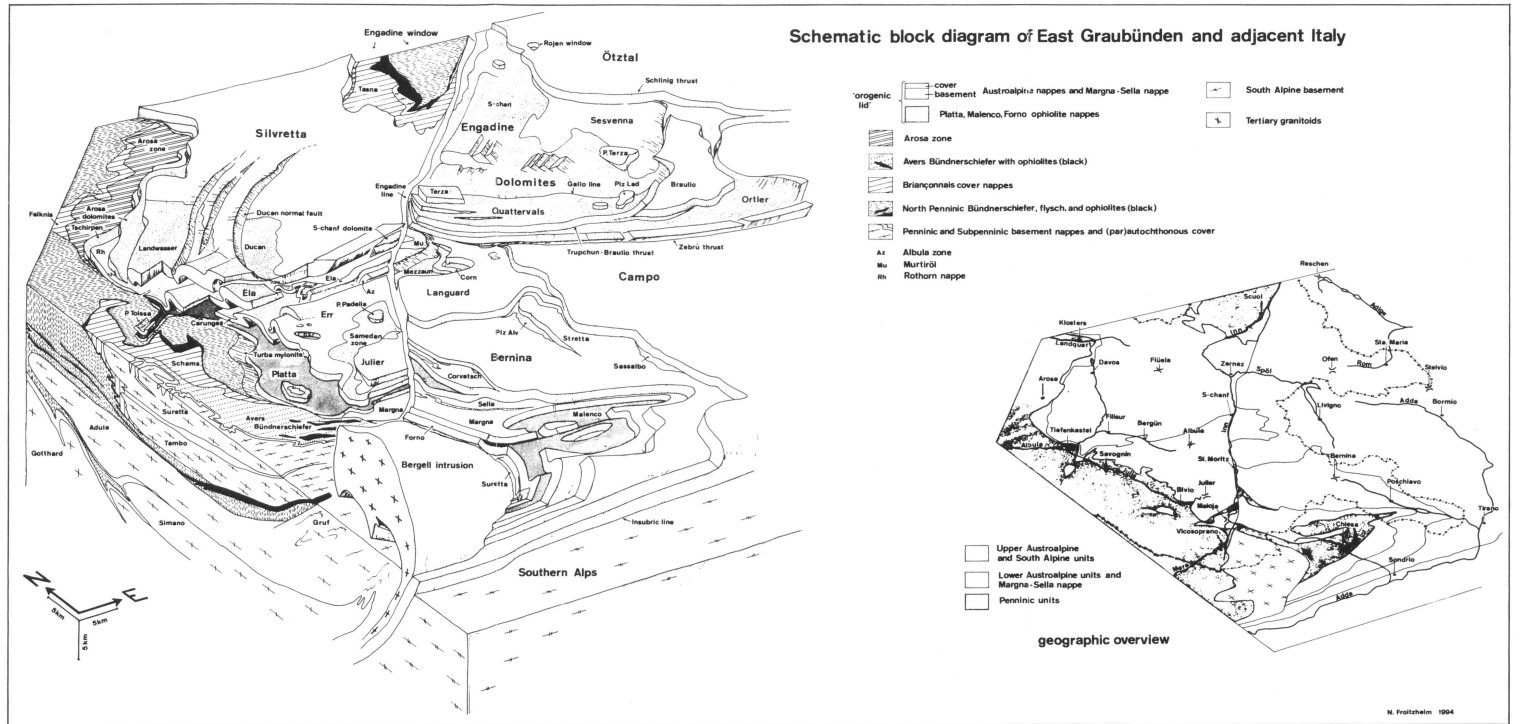
- SCHMID, S. M. & HAAS, R. 1989: Transition from near-surface thrusting to intrabasement décollement, Schlinig thrust, Eastern Alps. *Tectonics* 8/4, 697–718.
- SCHMID, S. M., RÜCK, P. & SCHREURS, G. 1990: The significance of the Schams nappes for the reconstruction of the paleotectonic and orogenic evolution of the Pennine zone along the NFP-20 East traverse (Grisons, eastern Switzerland). *Mém. Soc. géol. France* 156, 263–287.
- SCHMID, S. M. & HANDY, M. 1991: Towards a genetic classification of fault rocks: Geological usage and tectono-physical implications. In: *Controversies in modern geology*. (Ed. by Müller, D. W., McKenzie, J. A. & Weissert, H.) Academic press, London etc., 339–361.
- SCHMID, S. M. & FROITZHEIM, N. 1993: Oblique slip and block rotation along the Engadine line. *Eclogae geol. Helv.* 86, 569–593.
- SCHREURS, G. 1993: Structural analysis of the Schams nappes and adjacent tectonic units: implications for the orogenic evolution of the Penninic zone in eastern Switzerland. *Bull. Soc. géol. France* 164, 415–435.
- SPICHER, A. 1972: Tektonische Karte der Schweiz, 1:500 000. Schweiz. Geol. Komm.
- SPILLMANN, P. 1993: Die Geologie des penninisch-ostalpinen Grenzbereichs im südlichen Berninagebirge. Diss. ETH Zürich Nr. 10175.
- SPITZ, A. & DYHRENFURTH, G. 1913: Ducan-Gruppe, Plessur-Gebirge und die Rhätischen Bögen. *Eclogae geol. Helv.* 12, 476–498.
- 1914: Monographie der Engadiner Dolomiten zwischen Schuls, Scans und dem Stilsjerjoch. *Beitr. geol. Karte Schweiz N. F.* 44, 1–235.
- STAUB, R. 1924: Der Bau der Alpen. Versuch einer Synthese. *Beitr. geol. Karte Schweiz N. F.* 52, 1–272.
- 1964: Neuere geologische Studien zwischen Bünden und dem oberen Veltlin. *Jber. natf. Ges. Graub.* 89–90, 1–217.
- STÖCKLIN, J. 1949: Zur Geologie der nördlichen Err-Gruppe zwischen Val d'Err und Weissenstein (Graubünden). Diss. Univ. Zürich.
- STUTZ, E. & WALTER, U. 1983: Zur Stratigraphie und Tektonik am Nordostrand der Engadiner Dolomiten am Schlinigpass (Gemeinden Sent, Graubünden und Mals, Südtirol). *Eclogae geol. Helv.* 76, 523–550.
- TERMIER, P. 1903: Les nappes des Alpes orientales et la synthèse des Alpes. *Bull. Soc. géol. France, série 4*, 3, 711–765.
- TIETZ, R., HANDY, M. R., VILLA, I. & KAMBER, B. 1993: Strukturgeologische und radiometrische Untersuchungen an der Grenze Unterostalpin-Penninikum im Raume Piz Lunghin und Piz dal Sasc (GR). Schweizerisches Tektonikertreffen Zürich, 26./27. 2. 1993, abstracts.
- THÖNI, M. 1980: Distribution of pre-Alpine and Alpine metamorphism of the southern Oetztal mass and the Scharl unit, based on K/Ar age determinations. *Mitt. geol. Ges. Wien* 71/72, 139–165.
- 1986: The Rb-Sr thin slab isochron method – An unreliable geochronologic method for dating geologic events in polymetamorphic terrains? *Mem. Sci. Geol. Univ. Padova* 38, 283–352.
- 1988: Rb-Sr isotopic resetting in mylonites and pseudotachylites: Implications for the detachment and thrusting of the Austroalpine basement nappes in the Eastern Alps. *Jb. geol. Bundesanst. (Wien)* 131, 169–201.
- THÖNI, M. & MILLER, J. A. 1987: ^{40}Ar - ^{39}Ar and Rb-Sr results from the Austroalpine sheet (abstract). *Terra cognita* 7, 93.
- THÖNI, M. & JAGOUTZ, E. 1993: Isotopic constraints for eo-Alpine high-P metamorphism in the Austroalpine nappes of the eastern Alps: bearing on Alpine orogenesis. *Schweiz. mineral. petrogr. Mitt.* 73, 177–189.
- TROMMSDORFF, V. & NIEVERGELT, P. 1983: The Bregaglia (Bergell) Iorio intrusive and its field relations. *Mem. Soc. geol. ital.* 26, 55–68.
- TRÜMPY, R. 1975: Penninic-Austroalpine boundary in the Swiss Alps: A presumed former continental margin and its problems. *Amer. J. Sci.* 275–A, 209–238.
- 1976: Du Pèlerin aux Pyrénées. *Eclogae geol. Helv.* 69, 249–264.
- 1977: The Engadine line: A sinistral wrench fault in the Central Alps. *Mem. geol. Soc. China* 2, 1–2.
- 1980: *Geology of Switzerland; a guide-book*. Wepf & Co., Basel.
- 1992: Ostalpen und Westalpen – Verbindendes und Trennendes. *Jb. geol. Bundesanst. (Wien)* 135, 875–882.
- TRÜMPY, R. & HACCARD, D. 1969: Réunion extraordinaire de la Société géologique de la France: Les Grisons. *C. R. Soc. géol. France* 1969 (9), 330–396.
- UNMÜSSIG, N. 1993: Tektonische und sedimentologische Untersuchungen der ostalpinen Ela-Decke rund um den Piz Uertsch, Graubünden. Unpubl. diploma thesis, Univ. Basel.
- WEH, M. 1992: Strukturgeologische und stratigraphische Untersuchung der Albula-Zone (Ostalpin) im Raum Preda, Kanton Graubünden. Unpubl. diploma thesis, Geol. Inst. ETH and Univ. Zürich.

- WERLING, E. 1992: Tonale-, Pejo- und Judikarien-Linie: Kinematik, Mikrostrukturen und Metamorphose von Tektoniten aus räumlich interferierenden aber verschiedenaltigen Verwerfungszonen. Diss. ETH Zürich Nr. 9923.
- WURSTER, D. 1991: Zur Geologie der südwestlichen Ducan-Gruppe (Silvretta-Decke). Unpubl. diploma thesis, Geol. Inst. ETH and Univ. Zürich.
- ZIEGLER, W. 1956: Geologische Studien in den Flyschgebieten des Oberhalbsteins (Graubünden). *Eclogae geol. Helv.* 49, 1–78.
- ZOEPPRITZ, K. 1906: Geologische Untersuchungen im Oberengadin zwischen Albulapass und Livigno. *Ber. natf. Ges. Freiburg i. Br.* 16.

Manuscript received September 17, 1993

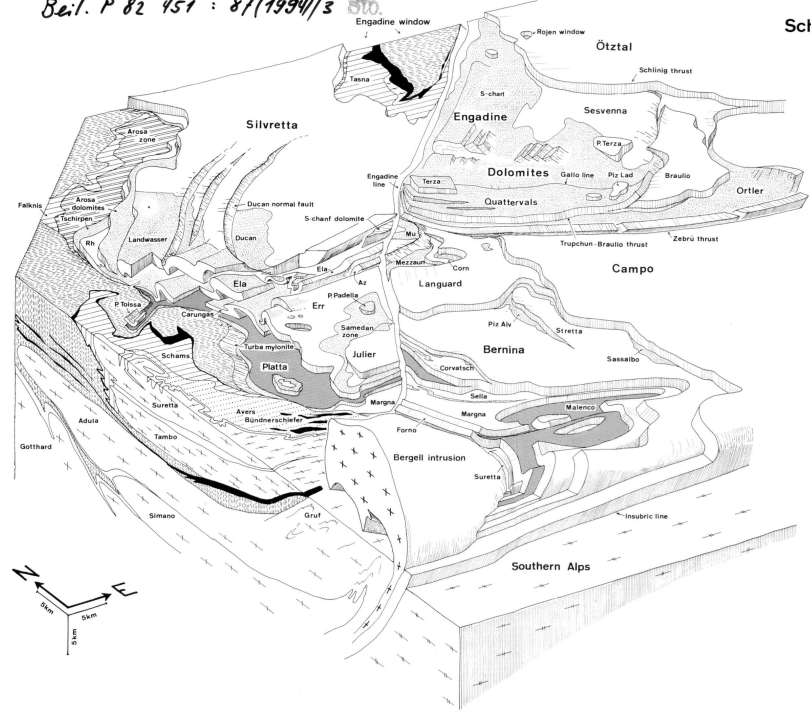
Revision accepted March 22, 1994

Plate 1. Schematic block diagram of East Graubünden and adjacent Italy.

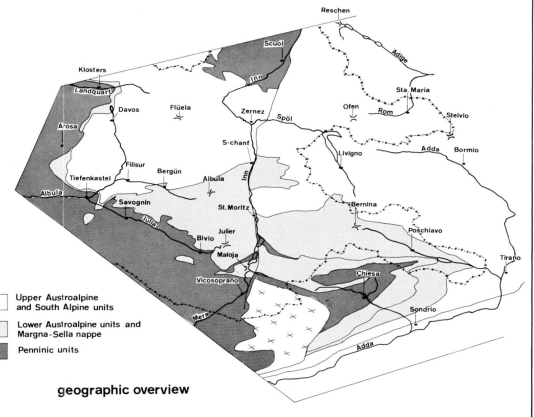


Beil. P 82 451 : 87(1994)/3 Sto.

Schematic block diagram of East Graubünden and adjacent Italy



- | | | |
|---|--|-----------------------|
| cover | Austroalpine nappes and Margna-Sella nappe | South Alpine basement |
| basement | Platta, Malenco, Forno ophiolite nappes | Tertiary granitoids |
| Arosa zone | Avers Bündnerschiefer with ophiolites (black) | |
| Briançonnais cover nappes | North Penninic Bündnerschiefer, flysch, and ophiolites (black) | |
| Penninic and Subpenninic basement nappes and (par)autochthonous cover | | |
| Az | Albula zone | |
| Mz | Murtöli | |
| Rh | Rothorn nappe | |



- | |
|---|
| Upper Austroalpine and South Alpine units |
| Lower Austroalpine units and Margna-Sella nappe |
| Penninic units |

geographic overview